NOVEL SILICA MEMBRANES FOR HIGH TEMPERATURE

GAS SEPARATIONS

A thesis

to

The Academic Faculty

By

Neha Bighane

In Partial fulfillment

Of the Requirements for the degree

Master of Science in the School of

Chemical & Biomolecular Engineering

Georgia Institute of Technology

May 2012

NOVEL SILICA MEMBRANES FOR HIGH TEMPERATURE

GAS SEPARATIONS

Dr. William J.Koros

School of Chemical and Biomolecular Engineering

Georgia Institute of Technology

Dr. Amyn Teja

School of Chemical and Biomolecular Engineering

Georgia Institute of Technology

Dr. Christopher Jones

School of Chemical and Biomolecular Engineering

Georgia Institute of Technology

ACKNOWLEDGEMENTS

I gratefully acknowledge the support and guidance of my advisor, Dr.Koros. Dr.Koros has provided me relentless backing through the progress of this project and also groomed my graduate career. I thank my committee members, Dr.Teja and Dr.Jones for their time, feedback, guidance and suggestions. The American Air Liquide', Inc. is thanked for providing financial assistance for this research. I also gratefully acknowledge the support of the Koros' research group members for invaluable suggestions and assistance.

I would like to acknowledge the Polymer Characterization Lab and the Laser Dynamics Lab at Georgia Tech for assistance with material characterization studies. I am also grateful to the KAUST foundation (award no. KUS-I1-011-21) for funding construction of the high temperature permeation system for my research. A special thanks goes to Ms.Michelle Martin for assistance with processing of my lab material orders and administrative issues, and Ms.Janice Whatley for administrative advising.

Table of Contents:

List of Tables

List of Figures

Summary

Membrane materials for gas separations span a wide range including polymers, metals, ceramics and composites. Our aim is to create economical hydrothermally stable membranes that can provide high H_2-CO_2 separation at a temperature of 300 degree Celsius, for application in the water-gas shift reactor process. The present work describes the development of novel silica and silica-titania membranes from the controlled oxidative thermolysis of polydimethylsiloxane. The scope of this thesis is fabrication of membranes, material characterization and preliminary gas permeation tests (35-80 degree Celsius) on PDMS derived silica membrane films. The developed membranes can withstand up to 350 degree C in air. High permeabilties of small gas penetrants like He, H_2 and CO_2 have been observed and fairly high separation factors of O_2/N_2=3, H_2/N_2= 14 and H_2/CH_4=11 have been obtained. As the temperature of operation increases, the permeability of hydrogen increases and the separation factor of H_2 from CO_2 increases. The silica membranes exhibit gas separation factors higher than the respective Knudsen values. Additionally, design and construction of a new high temperature gas permeation testing system is described, which will cater to gas permeation tests at temperatures up to 300 degree Celsius for future work. The thesis also includes a detailed plan for future studies on this topic of research.

Chapter 1. Introduction to Hydrogen Selective Silica Membranes

Introduction

Concern over supplies of oil and the steadily rising impact of global warming has driven tremendous interest worldwide in the development of hydrogen as an alternate fuel. The annual industrial **production of H_2** is 41MM tons (850 billion m^3 (STP) /year), which holds ~6Exajoules (1EJ= 10^{18} joules) or nearly 2% of the world's primary energy. Over 90% of this H_2 is generated from fossil fuel sources (mainly steam reforming of natural gas) [1].

There are three techniques known for H_2 separation and purification- 1) pressure swing adsorption (PSA), 2) fractional/cryogenic distillation and 3) **membrane separations**. While PSA involves high pressure adsorption (>10MPa) using suitable adsorbents, cryogenic distillation effects separation based on differences in boiling points of the gases. However, both these techniques are highly energy intensive processes. Membrane based separations work on the principle of a pressure driving force and preferential permeation of a single species from a gaseous feed mixture. Hence, membranes have the potential to provide 1) higher energy efficiency, 2) cost effectiveness, 3) simplicity in operation and 4) compactness and portability. Membrane technology can be coupled with existing steps in industrial production to improve overall efficiency of a process and increase throughput of the desired product. The motivation for my work stems from the need for the development of high performance cost effective gas separation membranes that can enhance the efficiency of hydrogen production (from natural gas) and separation process.

1.1 Water-gas shift reaction: Production of hydrogen from steam reforming of natural gas is the dominant H_2 production process. It comprises a highly endothermic steam-methane reforming

reaction (~800°C), a pair of water gas shift reactors (high temperature shift (HTS) at 350°C and low temperature shift (LTS) at 200°C) and downstream by-product CO_2 absorption unit [1-4].

In the steam reformer, natural gas reacts with high temperature steam (~800°C and 30-40 bar pressure with nickel catalysts) to produce syngas. Usually, complete conversion is achieved due to the high temperature and robust catalysts.

$$CH_4 + H_2O \leftrightarrow CO + 3H_2 \qquad \Delta H = 206 kJ/mol \qquad (1)$$

Additional H_2 is produced from a subsequent water gas shift reaction.

$$CO + H_2O \leftrightarrow CO_2 + H_2 \qquad \Delta H = -41.2 kJ/mol \qquad (2)$$

The water gas shift reaction (Equation 2) is thermodynamically limited and can be driven forward by selective removal of product hydrogen by membrane separation. Due to the exothermic nature of the reaction, lower temperatures favor conversion. *Installation of a H_2 selective membrane unit between the two water gas shift reactors can provide increased efficiency of the overall production process in the following ways:*

1. Production of a high purity commercial hydrogen stream from the membrane unit
2. Higher conversion in the LTS, due to lower concentration of products in the equilibrium mixture entering LTS
3. Higher rate of reaction in LTS, implying a smaller volume of reactor.
4. Excess reactant steam, that is currently used to drive the reaction forward, can be minimized
5. Product stream from LTS has been calculated to become CO_2 rich, as opposed to a H_2 rich stream in the absence of membrane separation, and downstream CO_2 capture becomes more efficient (Appendix I).

H_2 and CO_2 are the most abundant species in the equilibrium mixture exiting from the HTS, where the installation of the membrane unit is proposed. Typically, the product stream from a HTS operating at 350°C comprises 73.9% H_2, 17.7% CO_2, 7.4% CH_4 and 1.0% CO (dry basis) [1]. In addition to the gases, steam is also a major component in the reaction mixture. Hence, *it is necessary to seek the development of economical hydrothermally stable membranes that can provide high H_2/CO_2 selectivity at temperatures similar to the exit temperature of the HTS (300-350℃).*Hence, the overarching goal of my work is to develop stable and efficient H_2 selective membranes for separation after the first WGS reactor.

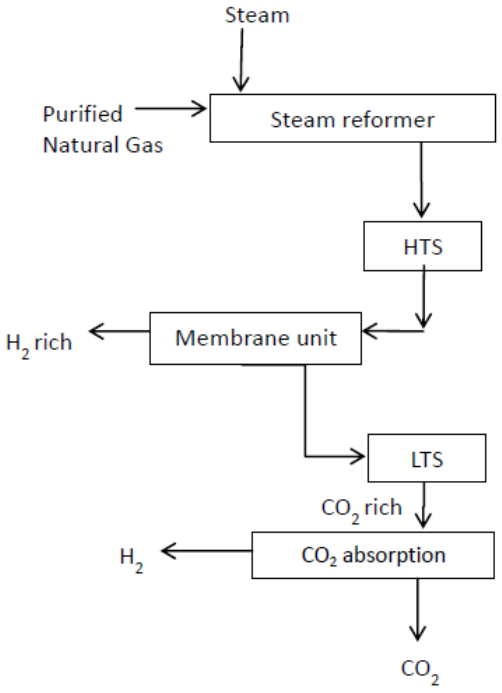

Figure i. Proposed process schematic of production of hydrogen from methane

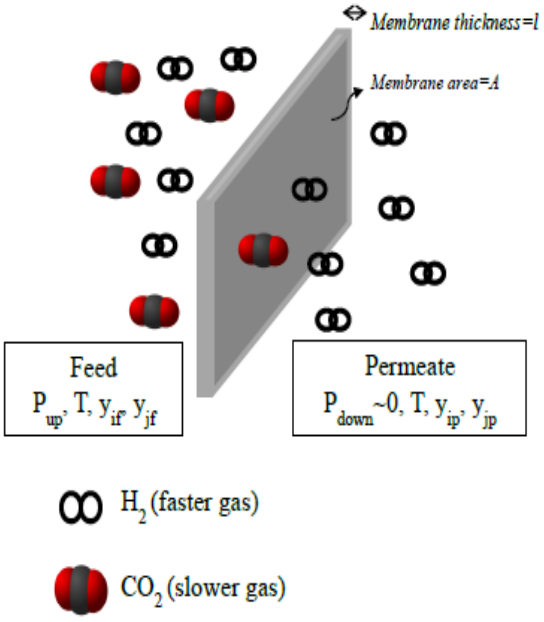

Figure ii. Cartoon of a membrane film that illustrates separation of H_2 from its mixture with CO_2

1.2 Literature on Silica membranes

A gas separation membrane is defined as a selective barrier between two gaseous phases. Owing to its microscopic structure and properties, it allows preferential passage of one of the components in a mixture under a partial pressure driving force. Characterization of membrane materials for gas separations primarily includes testing them for permeability (productivity) and selectivity (efficiency) towards the gases [7].

H_2 selective membrane materials span a wide range from dense metallics (pure metals like Pd and alloys) and inorganics (including zeolites, glasses and ceramics) to purely organic polymers and hybrid materials. Microporous amorphous silica membranes are promising candidates for hydrogen separations. Silica membranes exhibit high temperature stability in oxidizing

atmospheres. The efficiency of silica membranes is established and there are a number of publications on this subject [1-6].

There are two well-known techniques of preparing microporous silica membranes, namely, the Sol-Gel technique [3-4] and the Chemical Vapor Deposition (CVD) technique [8]. Both of these techniques require high-quality supports and CVD additionally requires high cost deposition reactors. While the Sol-Gel technique involves coating of liquid precursors on a support and subsequent heat treatment, CVD involves deposition of gaseous phase species on a support. A third technique of melt extrusion and leaching to make hollow fiber silica membranes (PPG Industries) was patented by Hammel et.al [9] and their gas transport properties were studied by many groups [5]. A fourth potentially low cost technique of making tubular silicon based membranes from a two-step calcination of silicone rubber tubes was explored by Lee and Khang [10]; however, the exact composition of the precursor tubes was not known and the membranes could not yield sufficiently good selectivities (i.e. above the Knudsen range). Nevertheless, this paper contributed to the idea which is the basis of the current work.

Table 1 presents a brief outline of some major research developments in this field for membranes prepared by the conventional methods, which do provide performance better than the Knudsen selectivity of 4.6 for H_2/CO_2.

Table 1. Major research found in literature, on permeation through silica membranes

Author(s)	Fabrication technique	Temperature in fabrication (°C)	Testing temperature(°C)	H_2/CO_2 selectivity
Nijmeijer (Thesis, University of Twente)[2]	Sol-Gel	600	200	45
		625	400	17
		625	600	21
Renate de Vos et.al. [3, 18]	Sol-Gel	600	300	70
	Sol-Gel (in clean room)	400	200	7
	Sol-Gel (in clean room)	600	300	98
J.D.Way et.al. [5]	Leaching	-	70	5.36

The siloxane bond (Si-O) is thermally stable and very resistant to homolytic cleavage because of its partially ionic and partially double bond character. The bond dissociation energy of Si-O is 101-118 Kcal/mol which is higher than that of the C-C bond (83 Kcal/mol) and comparable to the C-F bond (116 Kcal/mol) [12]. Therefore, silica membranes are a good choice for high temperature conditions.

Silica membranes are highly stable in dry oxidizing conditions at elevated temperatures and yield high H_2 selectivity over other larger gas molecules due to their microporosity; however, they exhibit an innate instability under hydrothermal conditions (high temperature steam). Condensation of surface silanol groups with hot steam causes densification and collapse of the

micropores, leading to loss in permeability and selectivity of smaller gas molecules over larger ones [13]. Available literature on sol gel reveals that silica membranes doped with inorganic metal oxides of B, Co, Ni, Ti, Zr, Al exhibit enhanced hydrothermal stability and gas separation properties [13-17]. The hypothesized cause of the stabilization is that the valence and coordination number of transition metal ions result in reduced interactions with –OH groups and prevents the structure of bulk silica matrix from altering in the presence of steam.

Hence, fabrication of hydrogen selective silica and silica-metal oxide membranes is the aim of the present research work.

1.3 Introduction to PDMS derived silica membranes

Due to the complexity of the conventional membrane fabrication processes for silica membranes, my work aimed to devise a more efficient and more economically scalable alternative silica membrane fabrication approach.

The concept of fabrication pursued here is based on careful optimization of the formation and thermal oxidation of a polysiloxane, viz., 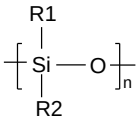

to silica (SiO_2), while retaining the mechanical integrity of the final film. Polydimethylsiloxane (R1=R2=-CH_3) is a liquid resin at room temperature. This resin is subject to chemical crosslinking using tetraethoxysilane ($Si(OC_2H_5)_4$). The crosslinked precursor is then thermally oxidized. The thermal oxidation step eliminates the organic side groups and stitches the polymeric chains together via oxygen, resulting in a silica membrane.

The thermo-oxidative stability of polysiloxanes [11] varies with the side groups as

$C_6H_5 > ClC_6H_4 > Cl_3C_6H_2 > Cl_2C_6H_3 > CH_2=CH > CH_3$

The precursor polymer was chosen as **polydimethylsiloxane or PDMS** (R1 = R2 = CH_3) due to i) its low cost, ii) availability of literature since it is the most widely studied polysiloxane and iii) because the methyl group is more easily oxidized as compared to other side groups.

1. This technique enables fabrication and testing of *unsupported* silica membranes (flat films) because the precursor is a solid rubbery film.

2. This approach allows the possibility of crosslinking PDMS with transition metal alkoxides, like titanium tetraethoxide, to obtain silica-metal oxide membranes. This latter capability is particularly attractive, since silica-metal oxide membranes are more stable in hydrothermal environments than pure silica matrices.

3. It has been experimentally observed that the fabrication parameters can be varied to tune the micromorphology of the silica membranes, and this is expected to provide considerable flexibility in creating tailored morphology for various applications in addition to high temperature H_2/CO_2 separation.

4. Finally, this fabrication technique holds the potential to enable its transformation into hollow fibers, which is the preferred membrane structure in industrial applications.

The scope of this thesis is fabrication (chapter 2), material characterization (chapter 3) and preliminary gas permeation tests (chapter 4) of PDMS derived silica membrane films. In addition, the design and construction of a high temperature permeation system is described (chapter 5), which will cater to gas permeation tests at temperatures up to 300°C for future work. Suggestions for future work are discussed in chapter 6. Appendix I presents calculations to demonstrate the advantages of installing a H_2-selective membrane unit in between the LTS and HTS, in the water-gas shift process. Appendix II is auxiliary to chapter 5 and presents heat transfer calculations.

References:

1. Ockwig, N.W. and T.M. Nenoff, *Membranes for hydrogen separation.* Chemical Reviews, 2007. **107**(10): p. 4078-4110.
2. Nenoff, T.M., R.J. Spontak, and C.M. Aberg, *Membranes for hydrogen purification: An important step toward a hydrogen-based economy.* Mrs Bulletin, 2006. **31**(10): p. 735-741
3. de Vos, R.M. and H. Verweij, *High-selectivity, high-flux silica membranes for gas separation.* Science, 1998. **279**(5357): p. 1710-1711
4. Arian Nijmeijer, *Hydorgen selective silica membranes for use in membrane steam reforming,* Ph.D. Thesis, University of Twente, 1999
5. Way, J.D. and D.L. Roberts, *Hollow Fiber Inorganic Membranes for Gas Separations.* Separation Science and Technology, 1992. **27**(1): p. 29-41.
6. Molyneux, P., *Permeation of gases through microporous silica hollow-fiber membranes: Application of the transition-site model.* Journal of Membrane Science, 2008. **320**(1-2): p. 42-56
7. Koros, W.J. and G.K. Fleming, *Membrane-Based Gas Separation.* Journal of Membrane Science, 1993. **83**(1): p. 1-80.
8. Gu, Y.F., P. Hacarlioglu, and S.T. Oyama, *Hydrothermally stable silica-alumina composite membranes for hydrogen separation.* Journal of Membrane Science, 2008. **310**(1-2): p. 28-37
9. Hassan, M.H., et al., *Single-Component and Mixed-Gas Transport in a Silica Hollow-Fiber Membrane.* Journal of Membrane Science, 1995. **104**(1-2): p. 27-42.
10. Kew-Ho Lee, Soon-Jai Khang, *Physical Characteristics of a porous silica material formed by pyrolysis of silicone rubber,* Ceram.Eng.Sci.Proc., 8 [1-2], pp.85-92, 1987
11. K.A. Andrianov, *Metalorganic Polymers,* Interscience publishers, 1965
12. Petar R. Dvornic, *High temperature stability of Polysiloxanes,* Silicon compounds: Silanes and Silicones Catalogue, Gelest Inc.
13. Boffa, V., D.H.A. Blank, and J.E. ten Elshof, *Hydrothermal stability of microporous silica and niobia-silica membranes.* Journal of Membrane Science, 2008. **319**(1-2): p. 256-263.
14. Kanezashi, M. and M. Asaeda, *Hydrogen permeation characteristics and stability of Ni-doped silica membranes in steam at high temperature.* Journal of Membrane Science, 2006. **271**(1-2): p. 86-93.

15. Yoshida, K., et al., *Hydrothermal stability and performance of silica-zirconia membranes for hydrogen separation in hydrothermal conditions.* Journal of Chemical Engineering of Japan, 2001. **34**(4): p. 523-530.
16. Kanezashi, M. and M. Asaeda, *Stability of H_2-permeselective Ni-doped silica membranes in steam at high temperature.* Jour nal of Chemical Engineering of Japan, 2005. **38**(11): p. 908-912.
17. Battersby, S., et al., *Hydrothermal stability of cobalt silica membranes in a water gas shift recator, Separation and Purification technology*, 2009. **66**: p. 299-305
18. R.M. de Vos, H. Verweij, *Improved performance of silica membranes for gas separation,* Journal of Membrane Science 143 (1998) 37-51
19. C.-Y. Tsai et al., *Dual-layer asymmetric microporous silica membranes,* Journal of Membrane Science 169 (2000) 255–268

Chapter 2. Fabrication of Silica Membranes from PDMS

This chapter describes fabrication of silica and silica-titania membranes from the controlled oxidative thermolysis of polydimethylsiloxane.

2.1 Fabrication of precursor: A precursor film of PDMS is cast on the basis of 'condensation cure' chemistry employing a solution casting method. Silanol (≡Si-OH) terminated polydimethylsiloxane was purchased from Gelest Inc. (DMS-S45, Mw= 80000-130000) and it is a viscous liquid at ambient conditions. A solution of the polymeric resin in n-heptane is thoroughly mixed with an appropriate crosslinking agent, tetraethoxysilane ($Si(OC_2H_5)_4$) (TEOS). A 5:1 weight ratio of PDMS to $Si(OC_2H_5)_4$ was found optimal, and 12-15mg of tin (di-n-butylacetoxytin 95%) and titanium (titanium-2-ethylhexoxide) catalysts, per gram polymer, were used to make a solution. The PDMS:TEOS ratio of 5:1 was found to be optimum based on careful studies of the ratio, with the preferred value showing the best mechanical properties in the final silica membranes after the oxidative thermolysis process. (A 2:1 (PDMS:TEOS) ratio resulted in minute clusters of silica particles within the precursor films, due to self-crosslinking of excess TEOS. This caused the precursor to crumble upon oxidative thermolysis. Precursor films that deviate by more than 3% from the 5:1 value result in either substructure cracks or crumbling or breaking of the films upon oxidative thermolysis. Hence, the value 5:1 was chosen as optimal and precursors fabricated with this value yielded defect free silica membranes upon thermal oxidation).

The well-mixed solution was then poured into a circular teflon dish (solution casting), maintained in a sealed glove bag filled with N_2 and water vapor. Moisture accelerates the crosslinking rate of the condensation cure reaction. Hence, a controlled humidity level between **70-85%RH** (Omega HH311 humidity meter) at 20-22°C was maintained in the glove bag. When the solution is

exposed to this atmosphere, the silanol ends of the PDMS chains undergo condensation with the ethoxy groups of $Si(OC_2H_5)_4$ (Figure 1). The polymer begins to crosslink to form a film in 22-30 minutes. The system is allowed to equilibrate for 21 hours to yield a transparent rubbery film. The film is then peeled off the dish and dried in a vacuum oven at 100°C for 20 hours and 120°C for 11hours to ensure complete removal of solvent, by-product and volatile materials. The obtained PDMS films are typically 7.9-8.4mils thick (1mil=1/1000 inch).

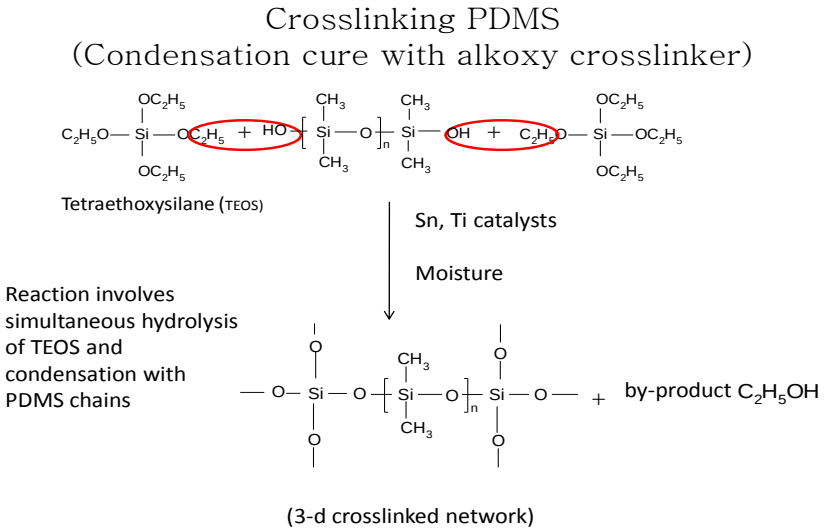

Figure 1. Schematic of TEOS crosslinking PDMS resin to obtain a rubbery PDMS film

2.2 Oxidative thermolysis: From the PDMS film obtained in the previous step, discs were cut and their weight, thickness and exact area (Scion Image) measured. To maintain uniformity, circles of ~5cm^2 area are punched out from the precursor PDMS film. These films were placed on a steel wire mesh inside a long quartz tube in a tubular furnace. The tube was sealed with an oxygen purge (99% O_2) at a desired flow rate (discussed later in Chapter 4). The system is heated

from room temperature to 390°C according to an optimized protocol (Table 2). The rubbery films undergo oxidative thermolysis to yield flat transparent silica membranes.

Table 2. Optimal temperature-time protocol for oxidative thermolysis of crosslinked PDMS films to silica membranes

Process Point	Process Point Value	Rate
Starting Setpoint	23 °C	
Set Point 1	250°C	
Time 1	1 hour 53 minutes	2°C/min
Set Point2	250°C	
Time 2	5 minutes	0°C/min (hold)
Set Point 3	390°C	
Time 3	1 hour 56 minutes	1.2°C/min
Set Point 4	390°C	
Time 4	15 minutes	0°C/min (hold)
Set Point 5	25°C	
Time 5	6 hours 5 minutes	1°C/min

The optimal time-temperature protocol for this thermal oxidation stage was obtained from a series of design experiments. First, it was observed that the precursor films do not undergo any weight loss (<0.5%) or change when subject to thermal oxidation up to 250°C under a pure oxygen purge. So, the initial ramp rate from room temperature to 250°C was set to a high value of 2°C/min.

Second, the flexible rubbery PDMS films get oxidized to silica films when subject to heat in oxygen up to 390°C and cooled. If heated beyond 390°C, the films begin to crack and crumble to

particles at 425°C (discussed in more detail in section 3.1). Hence, the maximum temperature was set to 390°C.

Third, variations in the ramp rate between 250 and 390°C led to change in the curvature of the silica films. A ramp rate of 1.5°C/min led to concave downward films and a ramp rate of 0.8°C/min led to concave upward films. Upon trial, it was observed that a ramp rate of 1.2°C/min yielded flat silica membranes. A soak time of 15minutes at 390°C and a cooling rate of 1°C/min were found to yield defect free silica membranes.

The final soak temperature must be high enough to ensure complete oxidation of the PDMS film; otherwise, an incompletely oxidized film (soak temperature 370°C) breaks during the cooling process due to difference in the thermal expansion coefficient of unoxidised PDMS and oxidized silica regions. The ramp rate determines the rate of oxidation of the film. Hence, curling of films is a function of rate of oxidation as this controls the relative percentage of oxidized and non-oxidized regions and the difference in the thermal expansion coefficients of regions inside the film.

Finally, the volumetric flow rate of oxygen in the purge was experimentally found to cause variations in the gas transport properties of the silica membranes which implies that the rate of mass transfer of O_2 to the oxidizing PDMS film causes variations in the pore size distribution of the final silica membranes. This is discussed in Chapter 4 and is important as it would allow tuning of the micromorphology of the membranes in future. O_2 flow rates of 30 and 50ml/min have been investigated. Higher concentration of O_2 leads to formation of smaller decomposition products (CO_2 and H_2, figure 2) and passage of these smaller molecules would yield smaller pores in the membrane.

At the end of the heating stage (set point 4 in table 2), the oxygen flow is stopped and the system cooled at 1°C/min. The accurate continuous flow of oxygen during the heating phase is important to complete the oxidation process as well as to purge out decomposition products. While the thermal program given in Table 2 was found to be optimum, some flexibility in the protocol may be tolerated; however, the stated conditions are recommended to prevent curling of the membranes, which complicates gas permeation masking and testing.

During the thermal oxidation stage, the methyl groups in the PDMS film undergo homolytic cleavage by gaseous phase O_2 and the siloxane free radicals from different chains are bridged via oxygen to form a three-dimensional silica matrix, and so internal rearrangement and shrinkage occurs. A schematic of the hypothesized mechanism [1, 2] is presented in figure 2.

Based on the mechanism shown in figure 2, the expected total weight loss in the thermal oxidation step can be theoretically calculated. Specifically, *removal of two methyl groups and addition of two half oxygen atoms (O shared by two Si) per unit PDMS should show an expected weight loss equal to*

$$= \frac{\left(-(2*15)+(2*0.5*16)\right)*100}{74} = 18.92\%$$

The experimentally observed weight loss of >20 samples was found to be 19±2%, which is in good agreement with the theoretical value. This indicates complete oxidation of PDMS to form a silica film. On an average, approximately 23% increase in the density of the material is observed upon oxidative thermolysis of PDMS. The area shrinks by ~31% and thickness decreases by ~6%.

It is also postulated that a very low or very high O_2 flow rate results in incomplete oxidation of the precursor. A very low O_2 flow rate would result in lack of sufficient mass transfer for thermal

oxidation. At very high O_2 flow rate, the outer layers of the precursor would undergo oxidation to form a layer so dense that they would hinder transport of O_2 to the inner layers. Both of the above conditions manifest as substructure cracks in the membranes or complete breaking of the films, upon thermal oxidation. Hence, variation in O_2 flow rate is a parameter that needs investigation.

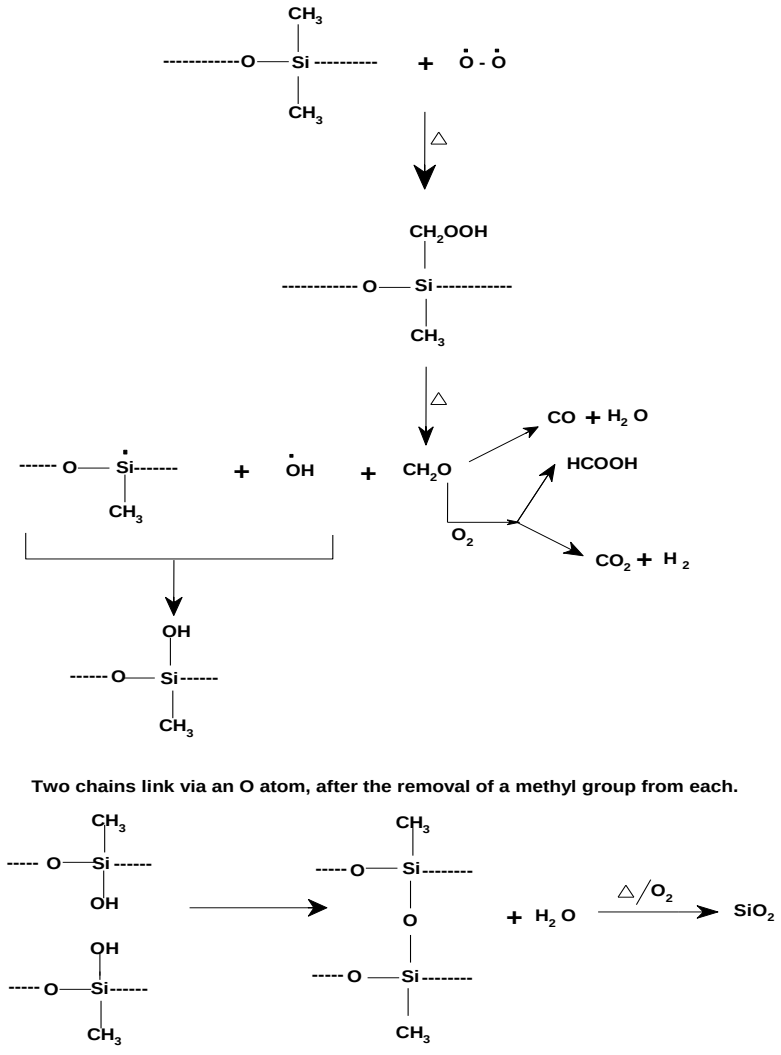

- Petar R. Dvornic, High Temperature Stability of Polysiloxanes, Silicon Compounds: Silanes and Silicones. Gelest. Inc.

Figure 2. Oxidative thermolysis of PDMS to silica

In this manner, silica membranes were fabricated from PDMS precursor films.

2.3 Fabrication of Silica-Titania membranes

As discussed in section 2.1, TEOS ($Si(OC_2H_5)_4$) was used to crosslink high Mw PDMS and obtain a rubbery PDMS precursor film. Instead of TEOS, when **titanium tetraethoxide ($Ti(OC_2H_5)_4$)** is used, Ti gets embedded as the crosslinks in the PDMS chains. This process yields *a rubbery Ti-crosslinked PDMS film which can be thermally oxidized to obtain silica-titania membranes.*

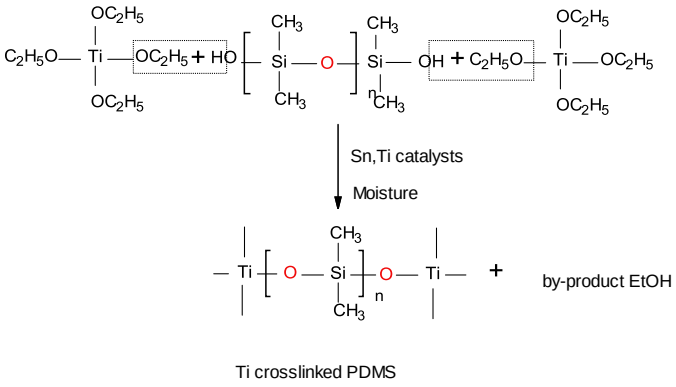

Figure 3. Schematic of crosslinking PDMS resin with titanium tetraethoxide, to form a rubbery Ti-crosslinked PDMS film

2.3.1. Casting precursor PDMS-TiO: The precursor PDMS-TiO is cast in a smooth circular Teflon® dish using solution casting similar to described in section 2.1. PDMS: $Ti(OC_2H_5)_4$ ratio = 5:1, solvent n-heptane, 12-15mg of tin (di-n-butylacetoxytin 95%) and 12-15mg of titanium (titanium-2-ethylhexoxide) catalysts, per gram polymer, are used to make a solution. The well-mixed solution is poured into a dish maintained in a glove bag, filled with N_2 and water vapor. Moisture greatly accelerates the rate of crosslinking of PDMS with $Ti(OC_2H_5)_4$. Hence, the humidity level maintained in the glove bag is **60-65%RH**. With this humidity range, PDMS gets crosslinked in 7-13 minutes to obtain a rubbery film of Ti-crosslinked PDMS (figure 3). The

system is allowed to equilibrate for 21 hours. The film is then peeled off the dish and dried in a vacuum oven at 100°C for 20 hours and 120°C for 11hours to ensure complete removal of solvent, by-product and volatile materials. The obtained PDMS films are typically 6.3-6.8 mils thick (1mil=1/1000 inch). A humidity level higher than 70%RH leads to a very high rate of crosslinking and leads to formation of patchy areas instead of a uniform integral film in the Teflon dish. The expected cause is the very high hydrolysis rate of titanium tetraethoxide with the silanol groups.

Note: One film was cast at 9%RH i.e. in pure N_2 atmosphere without any moisture. This film took 1 hour to crosslink. SiO-TiO membrane fabricated from this precursor film (as discussed in 2.3.2) was subject to preliminary gas permeation tests as reported in Chapter 4 (section 4.2). This exercise was carried out to test the inherent gas transport properties of silica-titania membranes.

2.3.2. Oxidative thermolysis: From the PDMS-TiO film obtained in the previous step, discs are cut and their weight, thickness and area (Scion Image) measured. To maintain uniformity, discs of ~5cm^2 area are punched out of the precursor film. These films are placed on a steel wire fine mesh inside a long quartz tube in a tubular furnace. The tube is sealed with an oxygen purge (99% O_2) at a desired flow rate. The system is heated from room temperature to 410°C according to an optimized protocol (table 3). The critical ramp rate is 0.5°C/min to yield flat membranes. The rubbery films undergo oxidative thermolysis to yield flat glossy transparent films of SiO-TiO. At the end of the heating stage (set point 4 in table 3), the oxygen flow is stopped and the system cooled at 1°C/min. The accurate continuous flow of oxygen during the heating phase is important to complete the oxidation process as well as to purge decomposition products. An initial ramp rate 2°C/min to soak at 150°C is used as the precursor film does not undergo any

modification until this temperature. The thermal degradation begins at 150°C in Ti containing PDMS films due to evolution of volatile cyclic oligomers.

Table 3. Optimal temperature-time protocol for oxidative thermolysis of Ti crosslinked PDMS films to Silica-Titania membranes

Process Point	Process Point Value	Rate
Starting Setpoint	23 °C	
Set Point 1	150°C	
Time 1	1 hour 2 minutes	2°C/min
Set Point2	150°C	
Time 2	5 minutes	0°C/min(hold)
Set Point 3	410°C	
Time 3	8 hour 40 minutes	0.5°C/min
Set Point 4	410°C	
Time 4	15 minutes	0°C/min(hold)
Set Point 5	25°C	
Time 5	6 hours 25 minutes	1°C/min

During the thermal oxidation stage, the methyl groups in the PDMS film undergo homolytic cleavage by gaseous phase O_2 and the siloxane free radicals from different chains are bridged together via oxygen (figure 2) to form a three-dimensional TiO-SiO matrix. Internal rearrangement and shrinkage occurs.

On an average from 15 samples, when PDMS-TiO gets thermally oxidized to SiO-TiO, Weight loss = 43%, shrinkage= 34%, decrease in thickness= 22%, increase in density=25%.

Like in the case of formation of pure silica membranes, Ti-crosslinked PDMS also oxidizes by removal of methyl groups and inter-chain bond formation. However, the markedly high weight

loss of 43% as compared to 19% during formation of pure silica films is due to increased tendency of the material to degrade via formation of volatile cyclic oligomers. The electropositivity of Ti makes the crosslink bonds in PDMS particularly strong and this increases the tendency of the connected chain(s) to form volatile oligomers when subject to heat. This also indicates that intrinsically SiO-TiO membranes would possess a more permeable structure than pure silica membranes.

It must be noted that in this technique of fabrication, Ti gets chemically bonded into the silica matrix and leads to the existence of a single phase in the material. This provides structural stability and improved material properties. Sometimes, in the conventional Sol-gel technique, metal oxide fine particles are dispersed into a silica sol and cast into a composite membrane, which causes problems due to differences in thermal expansion coefficient between the silica and dispersed metal phase during oxidative thermolysis and hinders reproducibility in membrane fabrication.

This chapter, thus, described the fabrication methodology of converting PDMS films to silica[6] or silica-titania membranes.

References:

1. Petar R. Dvornic, *High temperature stability of Polysiloxanes,* Silicon compounds: Silanes and Silicones Catalogue, Gelest Inc.
2. K.A. Andrianov, *Metalorganic Polymers,* Interscience publishers, 1965
3. Kew-Ho Lee, Soon-Jai Khang, *Physical Characteristics of a porous silica material formed by pyrolysis of silicone rubber,* Ceram.Eng.Sci.Proc., 8 [1-2], pp.85-92, 1987
4. Shingo Katayama et.al, *Characterization and Mechanical Properties of Flexible Dimethylsiloxane-Based Inorganic/Organic Hybrid Sheets,* J. Am. Ceram. Soc., **85** [5] 1157–63 (2002)

5. Silanes and Silicones, Gelest Catalogue 4000-A
6. N.Bighane, W.J.Koros, *Novel Silica membranes for high temperature gas separations,* Journal of Membrane Science, 371 (2011) pp.254-262

Chapter 3. Material Characterization

3.1 Thermogravimetric analysis: Thermogravimetric analysis (TGA) is a thermal characterization technique in which a sample is subject to heat according to a known protocol, in an inert or oxidizing atmosphere, to observe its thermal degradation pattern. TGA in an air purge was employed to visualize the weight loss pattern during the oxidative thermolysis of crosslinked PDMS to silica. An open pan TGA was used to ensure complete exposure to the oxidizing atmosphere. Air was used instead of oxygen due to safety concerns for the test equipment. The sample was a crosslinked PDMS film and it was subject to heat up to 500°C under the air purge (Figure 4 a).The thermal protocol followed was the same as presented in table 2, up to 390°C. The ramp rate from 390°C to 500°C was also 1.2°C/min. The weight loss pattern obtained was an indicator of the conversion.

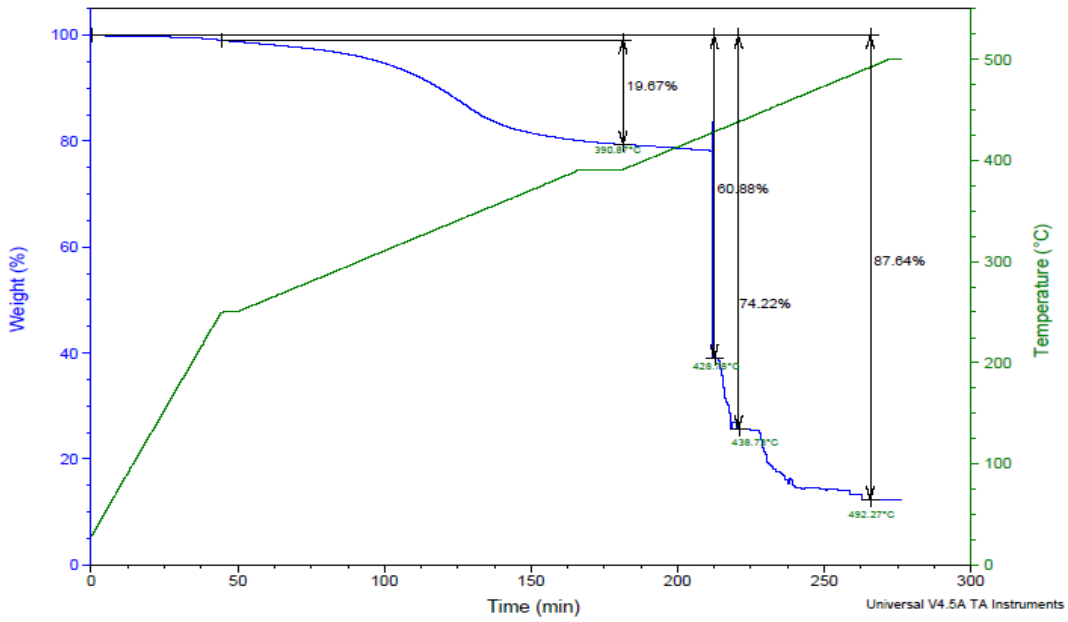

Figure 4a). TGA of crosslinked PDMS film in air

The first weight loss step begins from ~250°C and stabilizes at 390°C. Further heating to 425°C disintegrates the film into particles. From this observed weight loss pattern, it is clear that the conversion of PDMS to silica is complete by 390°C as the weight loss reached the theoretical value of ~19% and the film was intact until this temperature. The same was observed in the actual fabrication process as discussed in section 2.2. Beyond 425°C, breakdown of the Si-O bonds and redistribution (i.e. splitting and reforming) occurs to form volatile oligomers and a residue of fine silica particles [1]. This indicates a phase transformation in silica beginning after 390°C that encourages grain formation.

Second, TGA was used to verify the thermal stability of the silica membranes. It was observed that the films are thermally stable at 390°C in air for two hours (dry oxidizing condition) (figure 4b). *Consequently, the membranes can easily withstand a temperature of 300-350℃, as desired for application in the water gas shift process.*

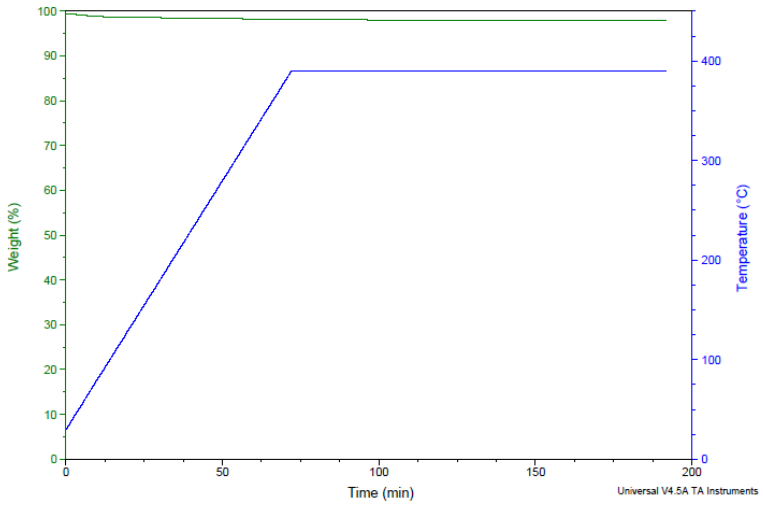

Figure 4b) TGA of silica film in air showing no weight loss at 390°C in a 2 hour test

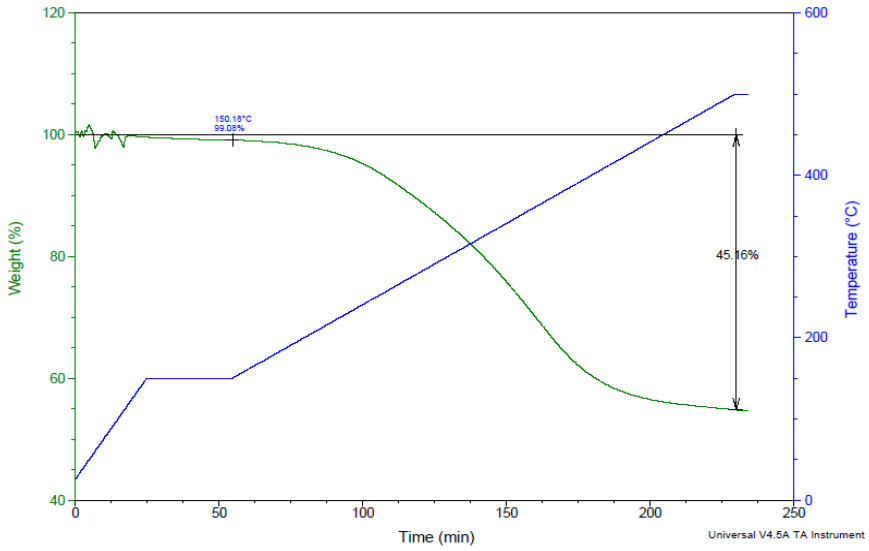

Figure 5a) . TGA of Ti-Crosslinked PDMS, in an air purge

TGA was also employed to investigate the weight loss pattern when Ti-crosslinked PDMS is subject to thermal oxidation in air. Thermal program was 2°C/min ramp rate from 150 to 500°C. The obtained result (figure 5) shows that the process is a one step weight loss beginning at 150°C and stabilizing at 410°C until when the film remains intact. This reveals that the induction of titanium into SiO helps enhance the thermal stability to 410°C, 20°C higher than pure SiO_2 (390°C is the maximum temperature for pure SiO_2 membranes) i.e. a retardation of the phase transformation to a higher temperature. The weight loss is ~45% due to removal of organic groups as well as formation of volatile oligomers.

The electropositivity (tendency to donate electrons) of Ti is -1.5 and that of Si is -1.9. Replacement of some Si-O linkages with Ti-O results in a more ionic bond due to higher electropositivity of Ti and the overall membrane film becomes stronger. The high weight loss is due to formation of volatile cyclic oligomers but the entire system oxidizes such that the film remains unbroken until 410°C. When two bonds are broken to form a volatile cyclic oligomer, the

bonds join immediately and the SiO-TiO matrix remains intact (shown in the following schematic).

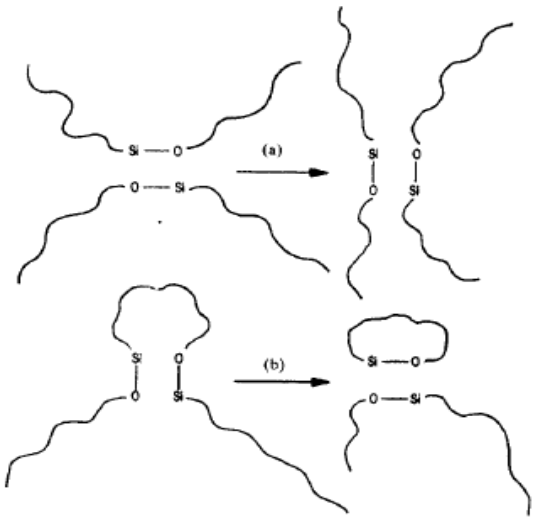

Figure 5b). Re-arrangement for bonds and formation of volatile cyclic oligomers during thermal degradation of a polysiloxane [2]

3.2. Fourier Transform Infra-red Spectroscopy: Fourier transform infrared spectroscopy (FTIR) is a characterization technique in which exposure of a sample to an IR beam yields characteristic peaks of various chemical bonds present in the sample. FTIR was employed to investigate the chemical structure of the precursor PDMS films and final silica membranes. The obtained absorbance spectra along with description of characteristic peaks are shown in Figures 6a) & b).

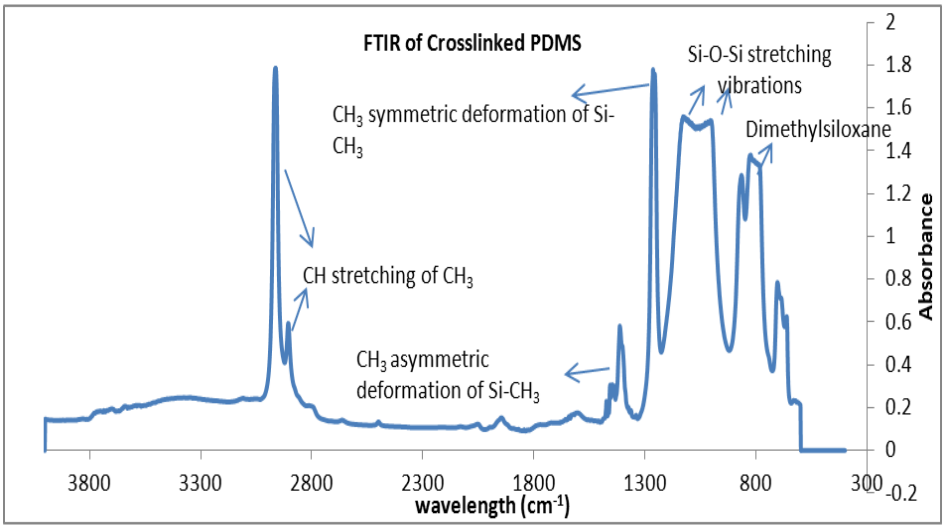

Figure 6a) FTIR of crosslinked PDMS precursor thin film

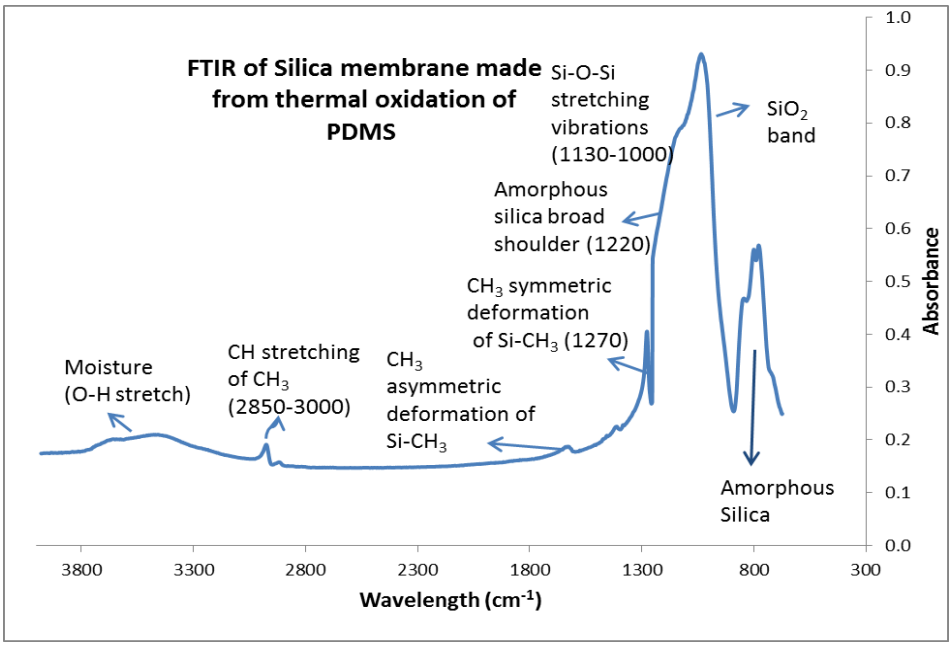

Figure 6b) FTIR of silica membrane (KBr pellet technique)

The large reduction in the methyl peak (2970cm^{-1}) and the evolution of the broad shoulder between 1000 and 1250cm^{-1} that is a signature of amorphous silica, in figure 6b) relative to figure 6a) demonstrate the transformation of PDMS to silica via thermal oxidation.

FTIR was also used to investigate chemical bonds in Ti-crosslinked PDMS precursor and derived SiO-TiO membrane (Figures 7 a) and b)).

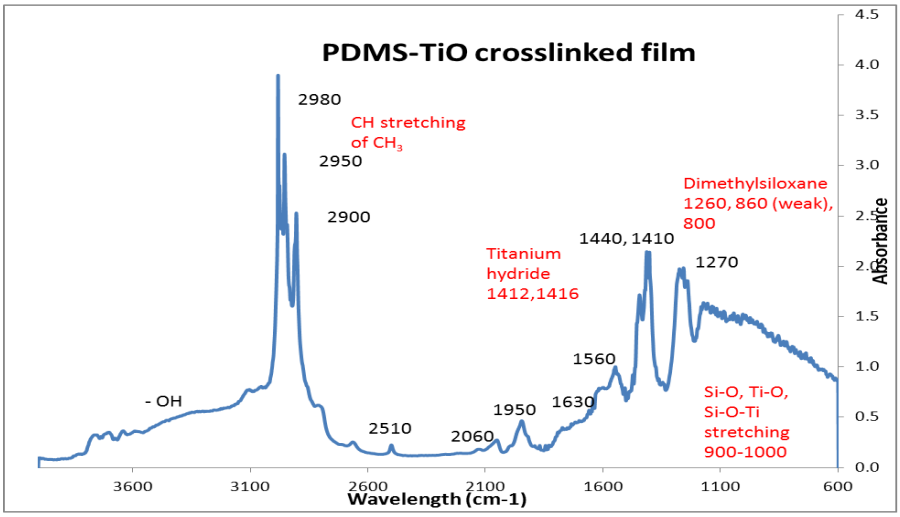

Figure 7a) FTIR of Ti-crosslinked PDMS precursor film

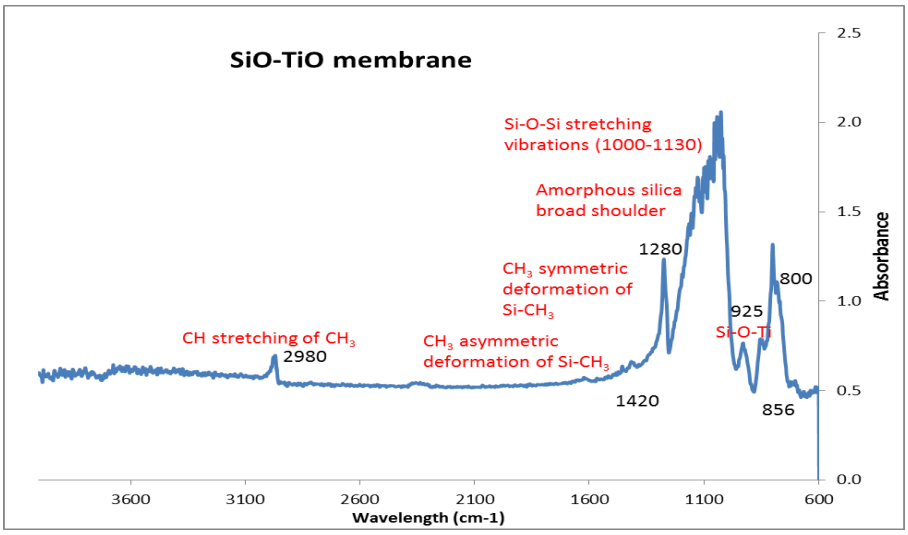

Figure 7b). FTIR of SiO-TiO membrane (KBr –pellet technique)

In figure 7a), characteristic peaks for Si-O-Ti (925-980cm^{-1}) [2, 7-8], Ti-O (933cm^{-1}), Si-O (1000-1130) and Si-CH_3 (1270-1290cm^{-1}) are seen. This confirms the bonding of Ti into PDMS

as crosslink points. The obtained peaks in figure 7b), which is the FTIR of derived SiO-TiO membrane, reveal the characteristic SiO shoulder (1000-1130cm^{-1}) and the presence of Ti bonded in the silica matrix (925 cm^{-1}). The area under the TiO peak at 925 cm^{-1} was 11% of the area under this peak and the SiO broad shoulder (Sigmaplot). Thus, as a first approximation, it is estimated that there is 11% Ti in the SiO-TiO membrane. Elemental chemical analysis would provide more accurate chemical composition.

Thus, TGA and FTIR were two characterization techniques used to validate the process of fabrication of PDMS derived silica and silica-titania membranes. These technqiues also helped determine the thermal properties and chemical structure of the silica membranes.

References:

1. K.A. Andrianov, *Metalorganic Polymers,* Interscience publishers, 1965
2. Silanes and Silicones, Gelest Catalogue 4000-A.
3. G.Camino, et.al., *Polydimethylsiloxane thermal degradation Part 1. Kinetic aspects*, Polymer 42 (2001) 2395-2402.
4. G.Camino, et.al., *Thermal polydimethylsiloxane degradation Part 2.The Degradation mechanisms*, Polymer 43 (2002) 2011-2015.
5. Young-Seok Kim, et.al, *Preparation of Microporous Silica Membranes for Gas Separation,* Korean J. Chem. Eng., **18**(1), 106-112 (2001)
6. J. Sekulic, et.al., *Microporous silica and doped silica membrane for alcohol dehydration by pervaporation*, Desalination 148 (2002) 19-23
7. Bunjerd Jongsomjit, et.al., *Catalytic Activity During Copolymerization of Ethylene and 1-Hexene via Mixed TiO2/SiO2-Supported MAO with rac- Et[Ind]2ZrCl2 Metallocene Catalyst*, Molecules 2005, 10, 672-678

8. Yue Chunxiao, et.al., Effect of Ti doping on microstructure of SiO2-CTAB mesoporous films, Journal of Physics: Conference Series **188** (2009)

Chapter 4. Gas separation performance of membranes

4.1 Theory and background

A gas separation membrane is defined as a selective barrier between two gaseous phases. Owing to its microscopic structure and properties, the membrane allows one of the gases, from a mixture, to permeate through faster than the other(s) under a partial pressure gradient. The intrinsic separation performance of a membrane material is measured in terms of its productivity (permeability) and efficiency (selectivity) [1]. Permeability, P, of a gas 'i' through a membrane is defined as the flux normalized by the partial pressure driving force.

$$P_i = D_i \cdot S_i = \frac{(\text{Flux})_i}{\Delta p_i / l} \qquad (3)$$

Permeability is related to the product of the diffusivity (dependent on molecular size) and the sorption capacity (dependent on condensability) of the penetrant gas molecule in the membrane. P_i is the permeability of gas i, through the membrane, Δp_i is the partial pressure difference of gas i across the thickness of the membrane and l is the thickness of the membrane. Permeability is a function of operating temperature and pressure (at the upstream and downstream) of the membrane, for a given membrane material, and is a measure of the intrinsic productivity of the membrane material. The unit of permeability commonly used is Barrer, which can also be expressed in SI units, viz.,

$$1\,\text{Barrer} = 10^{-10}\,\frac{\text{cm}^3(\text{STP})\cdot\text{cm}}{\text{cm}^2\cdot\text{sec}\cdot\text{cm Hg}} = 3.348\times10^{-16}\,\frac{mol.m}{m^2.s.Pa} \qquad (4)$$

Gas permeation tests can be carried out with pure gases or mixed gases. The ratio of the permeabilites of pure gases, for negligible downstream pressure at the same temperature and upstream pressure, is defined as ideal selectivity or permselectivity. For a mixed gas feed, the separation factor of a membrane is the ratio of the concentrations in the permeate to that in the feed.

$$\alpha_{i/j} = \frac{\left(y_i / y_j\right)_{Permeate}}{\left(y_i / y_j\right)_{Feed}} \cong \frac{\boldsymbol{P}_i}{\boldsymbol{P}_j} = \frac{D_i S_i}{D_j S_j} \qquad (5)$$

The variation of permeability with temperature for a given feed partial pressure follows an apparent Arrhenius relationship, viz.,

$P=P_0 \exp [-E_p/RT]$ (6)

where P_0 is a pre-exponential factor, Ep is the apparent activation energy for permeation, T is the temperature in degree Kelvin and R is the Universal Gas constant.

$E_p= E_d + \Delta H_s$ (7)

The activation energy for permeation is the sum of the activation energy for diffusion and the heat of sorption (usually exothermic i.e. ΔHs is often a negative value). Hence, as temperature rises (constant Δp_i), the diffusivity of a penetrant in a membrane increases while its sorption capacity decreases. Accordingly, the permeability varies as per equation 6.

As pressure increases (constant T), permeability of a gas either decreases due to saturation in pore capacity for the penetrant or remains constant. The decrease in permeability with pressure is especially enhanced for highly condensable gases like CO_2 due to large reductions in penetrant sorption at elevated pressures.

It is generally recognized that gas transport through polymeric membranes is governed by the solution-diffusion mechanism [1], dependent on chain mobility and involving molecular

dissolution of the gas between polymeric segments. In inorganic porous membranes with rigid and stable pores, gases permeate through the open spaces; however, the mechanism of permeation is sorption-diffusion if the pores are small enough to achieve size discrimination between the sorbed molecules as they execute diffusive jumps [1-4].

The detailed diffusion mechanism in porous membranes is dependent upon the size of the pores relative to the size of the permeating gas and the mean free path of the penetrant (figure 8 a)). If the pores are large compared to the molecular size of the penetrants but small relative to the bulk gas mean free path under the conditions of measurement, Knudsen diffusion tends to be dominant wherein the gas molecules only collide with the pore walls. For Knudsen transport, the selectivity is low and equal to the inverse ratio of the square root of the molecular weight of the two permeating gases. For example, in the case of O_2 and N_2, the smaller but heavier O_2 permeates slower than N_2 by the factor $(28/32)^{1/2}=0.94$.

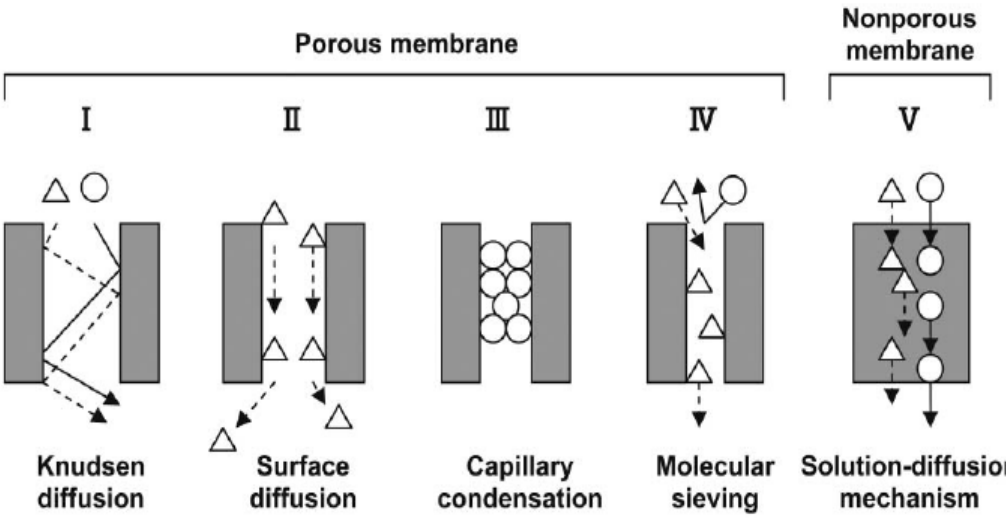

Figure 8a). Modes of gas permeation through porous and non-porous gas separation membranes; the mechanism varies from Knudsen in mesoporous to molecular sieving through ultra-microporous (r_p<5Å) membranes[12]

In microporous (r_p< 2nm) inorganic membranes such as the silica membranes considered here, the pores are of sizes of the order of the size of the penetrants, and interaction between the penetrant and the pore walls become significant, especially at low temperatures. Hence, in addition to diffusion through size selective pores, sorption becomes vital and the resultant mechanism becomes sorption-diffusion. In this case, the smaller O_2 permeates faster than N_2. The gas transport becomes thermally activated and shows molecular sieve-like separation properties, with high selectivities of small penetrants like He and H_2 over larger molecules. This has been observed in silica membranes fabricated using the Sol-Gel technique [2-10]. Figure 8b) presents the variation of permeability of five different gas penetrants through state-of-the art silica membranes prepared by the Sol-Gel technique [5]. As observed the permeability of all penetrants, except CO_2, increase with increase in temperature. CO_2 permeability decreases due to a decrease in its sorption (P=D.S) in the membrane with rise in temperature. High selectivities were obtained and gas penetrants larger than CH_4, like SF_6 (5.5Å) were completely sieved out i.e. could not permeate through the membrane.

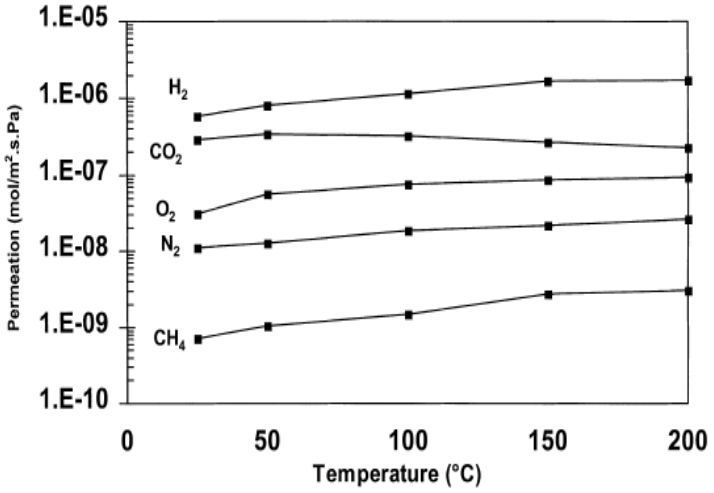

Figure 8.b) Temperature dependence of gas permeability for silica membrane fabricated by Sol-Gel technique [5]; fabrication temperature was 400°C.

For gases such as O_2 and N_2 that have similar sorption enthalpies, one can detect the onset of activated permeation when significant deviations from Knudsen selectivity become apparent. Thus, when the smaller but high molecular weight O_2 (3.46Å) permeates significantly faster than the slightly larger but lower molecular weight N_2 (3.64Å), activated sorption-diffusion is indicated. O_2-N_2 separation is difficult due to small difference in their molecular sizes. The case of H_2/CO_2 is more complex due to the high condensability of CO_2. CO_2 (3.3Å) can permeate faster than the smaller H_2 (2.89Å) due to high sorption, at low temperatures. But as temperature increases, the high diffusivity of H_2 starts dominating, the sorption of CO_2 decreases, and H_2 permeability starts increasing while that of CO_2 decreases.

4.2 Gas separation performance of Silica membranes

In this section, gas permeation data of six penetrants through PDMS derived silica membranes is presented in the temperature range 35-80°C. Higher test temperatures could not be attained due to constraints in the available permeation test system. For collection of the data presented in this chapter, silica membranes were masked into a stainless steel permeation cell using an aluminum foil tape (Fasson®, rated to 120°C) and Duralco® epoxy. Masking refers to attaching the membrane to the test cell such that the only available path for gas transport remains through the membrane. The epoxy is heat cured at 80°C for 4 hours. The permeation cell is then tightly enclosed and mounted into a permeation system in between an upstream section and downstream section. To provide the temperature of operation in the range 35-80°C, the upstream volume which holds the feed gas, its inlet connection to the permeation cell and the permeation cell were heat wrapped carefully using a heavy insulated heating tape. The heating was controlled using a K-type thermocouple and a PID benchtop controller. The remainder of the system, including the downstream, remained at ambient conditions (25-30°C) and its temperature was noted for

permeability calculations. Downstream pressure transducer collects permeation data of a gas through the membrane (rise of pressure due to accumulation of permeate in the downstream volume).

Variation in the O_2 flow rate, used during the fabrication of the PDMS derived silica membranes, results in variations in gas separation properties. Hence, two different values of O_2 flow rate fabrication parameter 30 and 50 ml/min were investigated. The gas permeability data is presented in figures 9, 10 and 11. High permeabilities of small penetrants like He, H_2 and CO_2 are obtained while larger penetrants like O_2, N_2 and CH_4 show permeabilities that are about 10 times lower. It would be expected that in permeation through a microporous membrane, a smaller penetrant would have higher permeability. But, the permeability of CO_2 was observed to be slightly higher than that of H_2 at 35°C, which indicates that in addition to molecular diffusion, selective sorption plays a significant role in the mechanism of permeation.

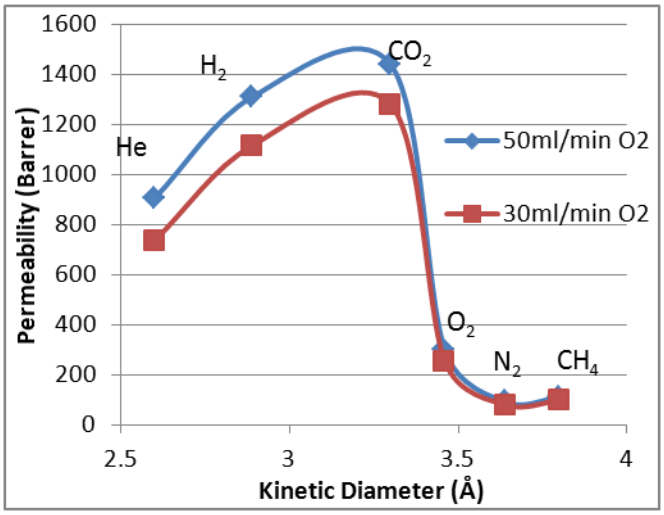

Figure 9. Permeability of silica membranes at 55.2psia, 35°C, for He, H_2, CO_2, O_2, N_2 and CH_4, fabricated with two different O_2 flow rate parameter values

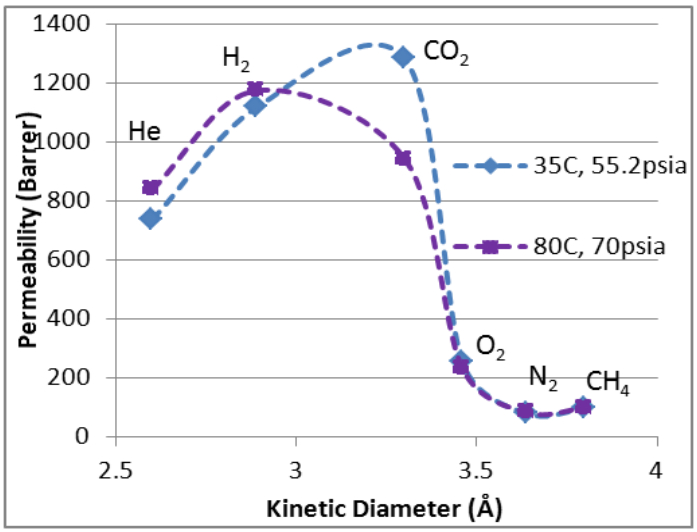

Figure 10. Permeabilites of He, H_2, CO_2, O_2, N_2 and CH_4, for a silica membrane (fabricated at 30ml/min O_2 flow rate) at 35°C, 55.2psia and 80°C, 70psia

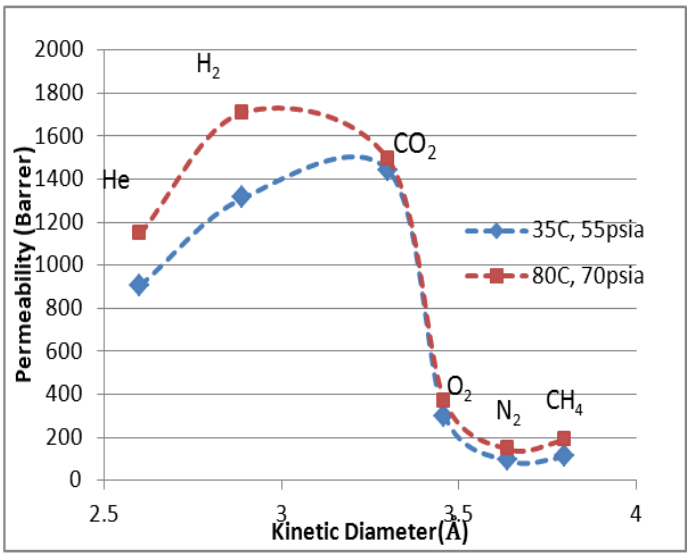

Figure 11. Permeabilites of He, H_2, CO_2, O_2, N_2 and CH_4, for a silica membrane (fabricated at 50ml/min O_2 flow rate) at 35°C, 55.2 psia and 80°C, 70psia

Table 4. Pure gas selectivites of PDMS derived silica membranes fabricated at different O_2 flow rates

Pure Gas Selectivity					
O_2 flow rate during fabrication	50ml/min		30ml/min		Knudsen Value
Feed conditions	35°C, 55.2 psia	80°C, 70psia	35°C, 55.2 psia	80°C, 70psia	
H_2/CO_2	0.91	1.15	0.87	1.25	4.69
O_2/N_2	3.3	2.6	3.2	2.8	0.94
H_2/N_2	14.5	11.9	14.0	14.1	3.74
H_2/CH_4	12.1	9.1	11.6	11.9	2.83
CO_2/CH_4	13.3	8.0	13.3	9.6	0.60
CO_2/N_2	16.0	10.4	16.0	11.3	0.80

As shown in figure 9, variation in the O_2 flow rate (during fabrication) leads to changes in the gas transport properties of He, H_2 and CO_2. It is hypothesized that smaller pores that are more selective to He and H_2 are obtained when a higher O_2 flow rate is used. Consistent with results for silica membranes created by sol-gel membrane preparation techniques in literature, the silica membranes appear to possess an interconnected network of pores and the pore size distribution is such that the smaller gas penetrants can access a larger fraction of the total pores. The average pore size of the majority of pores lies between the kinetic diameters of H_2 (2.89Å) and O_2 (3.46Å). Selectivity values higher than those expected from Knudsen range are obtained as tabulated in table 4, which leads to the assumption of the presence of ultra-micropores in the membranes.

The ideal separation factor for H_2/CO_2 increases from 0.87 (i.e. CO_2 selective) at 35°C, 55.2 psia to 1.25 (i.e. H_2 selective) at 80°C, 70 psia. It is particularly significant that the H_2/CO_2 selectivity has "switched" as the temperature rose by only 45°C. These data show the tendency to shift from a sorption dominated selectivity for the condensable CO_2 at 35°C to a size dominated selectivity for H_2 at 80°C. This trend in anticipated to become more extreme and strongly favor H_2 at still higher temperatures, which is desired. The O_2/N_2 selectivity is 3 and is reasonable given that a value between 3-8 is considered good for this tough separation as O_2 (3.46Å) and N_2 (3.64Å) are very similar in size. The combination of H_2 permeability of 1200Barrer and H_2/N_2 selectivity of 14 lies on its upper bound curve [11] for polymer membranes for this separation. A fairly high CO_2/CH_4 selectivity of 13 is also observed. The permeabilities of He, H_2, O_2, N_2 and CH_4 increase with increase in temperature while that of CO_2 decreases. This is indicative of activated nature of permeation with positive activation energies (E_p) except for CO_2, which has negative activation energy due to its sorption effects. In order to obtain data for accurate calculation of E_p's, it is important that data be collected over a wide temperature range (35-300°C). A new permeation test equipment (Chapter 5) has been designed and constructed to cater to gas permeation tests at temperatures up to 300°C. This task will be pursued in the future (chapter 6) and will enable compilation of data for permeabilities, selectivities and activated permeation parameters (E_p and P_0) of different gas penetrants.

Adsorption in silica membranes follows a Langmuir type mechanism and a type I adsorption isotherm is obtained which indicates monolayer adsorption of gases [5]. Figure 12 shows the variation of gas permeability, through PDMS derived silica membranes, with pressure from 50 to 100 psia, at 35°C. While the permeability of CO_2 (highly condensable) decreased by 11% with rise in Δp, the permeabilities of He, H_2 and N_2 remained constant. These data illustrate the effects

of isotherm curvature with pressure. CO_2 permeability decreases due to saturation in the sorption capacity of the membrane for the penetrant [1]. This fact also indicates that even at the low temperature of 35°C, the size based selectivity of the membranes for H_2 can be observed at high pressures. At 100 psia, the permeability of H_2 is higher than that of CO_2 at 35°C through silica membrane fabricated at 50ml/min O_2. Hence, it can be concluded from these results that *high temperatures and high pressures favor H_2 permeation over CO_2 through PDMS derived silica membranes.*

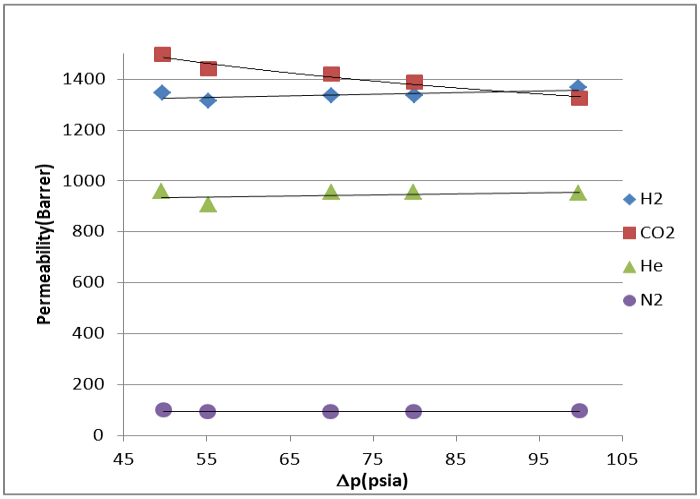

Figure 12. Variation of permeability of He, H_2, CO_2 and N_2, with pressure (50-100psia) at 35°C, of silica membrane fabricated at 50ml/min O_2

4.3 Discussion

The fabricated silica membranes were tested for permeability and pure gas selectivity with six gas penetrants- He, H_2, CO_2, O_2, N_2, CH_4. Two sets of experiments, one at 35°C, 55psia and the other at a higher temperature and pressure of 80°C, 70psia were conducted as shown in figures 10 and 11. With increase in temperature the permeabilities of all penetrants increased, except CO_2 whose permeability decreased. The expected cause for this exceptional behavior of CO_2 is its highly

sorbing nature which gives a high permeability (product of diffusivity and sorption coefficient) at 35°C but as temperature rises, its sorption coefficient decreases and the overall permeability decreases. H_2 (2.89Å) and CO_2 (3.3Å) have similar kinetic diameters. The small size of the H_2 molecule gives H_2 high diffusivity. However, lower critical temperature (T_c=33.2K) implies lower sorption capacity or condensability of H_2 compared to CO_2 (T_c=304.1K). In a H_2-selective membrane, the goal is to exploit the high diffusivity of H_2 and to limit the effect of high sorption of CO_2. In the present research also, it is expected that H_2/CO_2 selectivity will increase as temperature increases.

The permeabilities of small gas penetrants He, H_2 and CO_2 are an order of magnitude higher than that of larger penetrants like O_2, N_2 and CH_4. This is an indication of the pore size distribution in the silica membranes and it appears that the average pore size lies between the kinetic diameters of H_2 and O_2. There exist a very small fraction of larger pores through which N_2 and CH_4 can permeate and these large pores must be made smaller in order to achieve molecular sieving performance. If the average pore size can be shifted to a smaller value in between the kinetic diameters of H_2 and CO_2, very high H_2/CO_2 separation can be achieved. Pure gas selectivity values of the silica membranes were tabulated in table 4. The selectivity values were above the respective Knudsen range (inverse ratio of square root of Mw of gas pair), except for H_2/CO_2. The H_2/CO_2 selectivity increased from 0.87 at 35°C, 55psia to 1.25 at 80°C, 70psia. H_2/CH_4 drops from 12 at 35°C, 55psia to 9 at 80°C, 70psia in silica membranes created at 50ml/min O_2 but remains fairly constant in membranes made at 30ml/min O_2. The change in the permeabilities of the penetrants between 35°C, 55psia and 80°C, 70psia is slightly larger in silica membranes fabricated at 50ml/min. This indicates higher activation energies of permeation in the tighter pore structure of the membranes made at 50ml/min O_2. While the results provided first insight into the microporosity and gas separation abilities of the membranes, further research must be pursued in

order to obtain data of separation performance at higher temperatures. A temperature of 200-300°C must be investigated because in this range, sorption coefficients of the gases would be at their minimal value and size based selectivity values of PDMS derived silica membranes can be obtained.

As observed in figures 9-11, the O_2 flow rate is a key fabrication parameter and can be used to tune the micromorphology of the membranes. During the oxidative thermolysis stage, higher O_2 flow rate provides higher rate of mass transfer into the precursor film. At high concentration of O_2, smaller decomposition products are formed (figure 2) and hence, the pores formed due to the passage of these small products are smaller in diameter. The smaller pores are more selective to small gas molecules of He and H_2 than toward larger gases like O_2, N_2 and CH_4. From the data presented in figure 10, 11 and 12, it is already established that high temperatures and high pressures favor H_2 permeation over CO_2. Since H_2-CO_2 separation is the aim of this research, using an optimal value of the O_2 flow rate fabrication parameter can provide high separation factors. Additional fabrication parameters such as thermal ramp rate and final soak temperature may also be varied to alter the micromorphology of the silica membranes.

Gas permeation test on SiO-TiO membrane

As mentioned in a note in section 2.3, one Ti-crosslinked PDMS precursor was fabricated in a pure N_2 (no moisture, 9%RH, 1 hour crosslinking time) and this precursor was oxidized to SiO-TiO membrane film. It is expected that such a membrane would have large micropores because the crosslinking density of the precursor is low due to absence of moisture during its fabrication. This SiO-TiO membrane was tested to learn about the inherent differences that the presence of Ti can induce in a silica membrane.

Gas permeation tests were conducted on this SiO-TiO membrane in the temperature range 35-70°C with H_2 and CO_2. Variation in permeabilities was observed. Three data points (35, 50 and 70°C) were collected for each gas at Δp=49.7psia. Using these three data points, a plot of lnP (vs) 1/T was plotted. From this plot, the activation energy for permeation (measure of variation in permeability per unit change in temperature) and pre-exponential factor (permeability at very high temperature) were calculated (equation 6). These values were then used to estimate permeability values at higher temperatures. $P=P_0 \exp(-Ep/RT)$

Gas	Ep (kJ/mol)	P_0(Barrer)	$P_{estimated}$ (300°C, Barrer)
H_2	4.5	8804.34	3443.2
CO_2	-1.0	751.45	925.2
H_2/CO_2 selectivity at 300°C			3.72

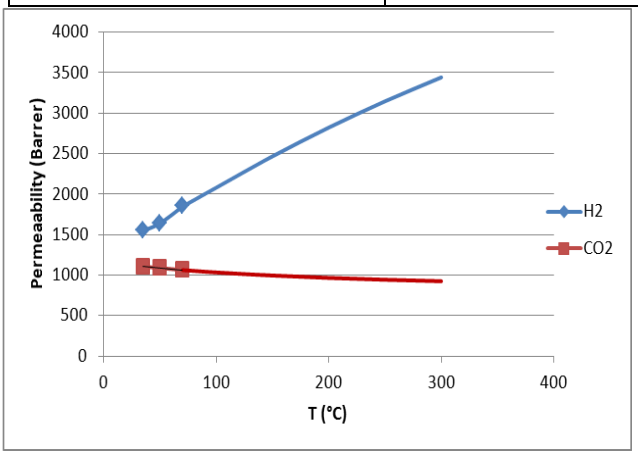

Figure 13. Estimated variation of permeability of SiO-TiO membrane with temperature, for H_2 and CO_2 at 49.7 psia (precursor fabricted without moisture, 9%RH)

This SiO-TiO membrane was observed to be H_2 selective, even at 35°C. This suggests that induction of Ti into SiO causes a change in the polarity of the bulk silica matrix so that the sorption of CO_2 is reduced compared to a pure silica membrane at 35°C (figure 9).

If the precusor has a high crosslink density (moisture during casting), the resultant SiO-TiO membranes will have smaller micropores and larger activation energies. This would yield high H_2/CO_2 selectivity at high temperatures. Hence,the above result is used as a proof of the efficacy of SiO-TiO membranes and future experiments on membranes fabricated with moisture crosslinked precursors is envisioned to provide high performance for H_2-CO_2 separations. Such membranes are also expected to be stable in the presence of steam.

Chapter conclusion:

From the gas permeation results presented in this chapter, it is concluded that

1. an appropriately processed polydimethylsiloxane sample can be converted in to molecularly selective silica membrane.

2. induction of titanium in a silica membrane provides altered material properties that enable additional engineering of the membrane material

The gas transport results obtained indicate an activated nature of transport through the microporous silica membranes. Fairly high selectivity values were obtained for 5 gas pairs and it was also observed that high temperatures and high pressures favor H_2 permeation over CO_2. To illustrate the utility of the newly developed silica membranes, it is essential to perform permeation tests at elevated temperatures. In order to conduct high temperature gas permeation tests, it is vital that the seal between the membrane and the test cell be leak proof. While the seals used in the work presented in this chapter had high integrity for measurements up to 80°C, difficulties in sealing above this temperature must be resolved. This task needs attention toward use of high temperature materials and construction of a high temperature permeation system is discussed in the following chapter 5. Chapter 6 describes future research to be pursued on the

PDMS derived silica membranes.

References:

1. Koros, W.J. and G.K. Fleming, *Membrane-Based Gas Separation,* Journal of Membrane Science, 1993. **83**(1): p. 1-80
2. Arian Nijmeijer, *Hydorgen selective silica membranes for use in membrane steam reforming,* Thesis, University of Twente, 1999
3. Molyneux, P., *Permeation of gases through microporous silica hollow-fiber membranes: Application of the transition-site model,* Journal of Membrane Science, 2008. **320**(1-2): p. 42-56
4. de Vos, R.M. and H. Verweij, *High-selectivity, high-flux silica membranes for gas separation.* Science, 1998. **279**(5357): p. 1710-1711
5. R.M. de Vos, H. Verweij, *Improved performance of silica membranes for gas separation,* Journal of Membrane Science 143 (1998) 37-51
6. Battersby, S., et al., *Performance of cobalt silica membranes in gas mixture separation.* Journal of Membrane Science, 2009. **329**(1-2): p. 91-98
7. Way, J.D. and D.L. Roberts, *Hollow Fiber Inorganic Membranes for Gas Separations.* Separation Science and Technology, 1992. **27**(1): p. 29-41
8. Hassan, M.H., et al., *Single-Component and Mixed-Gas Transport in a Silica Hollow-Fiber Membrane.* Journal of Membrane Science, 1995. **104**(1-2): p. 27-42.
9. Boffa, V., D.H.A. Blank, and J.E. ten Elshof, *Hydrothermal stability of microporous silica and niobia-silica membranes.* Journal of Membrane Science, 2008. **319**(1-2): p. 256-263
10. Barboiu, C., et al., *Structural and mechanical characterizations of microporous silica-boron membranes for gas separation.* Journal of Membrane Science, 2009. **326**(2): p. 514-525.

11. Benny D. Freeman, *Basis of Permeability/Selectivity Tradeoff Relations in Polymeric Gas Separation Membranes*, Macromolecules **1999,** 32, 375-380

12. John D. Perry, et.al., *Polymer membranes for hydrogen separation*, MRS Bulletin, Vol.31, October 2006, 745

Chapter 5. Construction of High Temperature Permeation System

There is growing interest in high temperature separations for application in H_2 separations using inorganic membranes. Characterization of membrane materials for various separations includes testing them for permeability (productivity) and selectivity (efficiency) towards the gases. Typically, such tests are performed in gas permeation testing systems at 35°C.

As mentioned in Chapter 4, gas permeation tests were performed on silica membranes in the temperature range 35-80°C. But, to demonstrate the actual utility of PDMS derived silica membranes, it is vital to collect gas separation data at elevated temperatures. For installation of a H_2-selective membrane unit at the exit of the HTS in water-gas shift process, the temperature of operation required is 300-350°C. Hence, this chapter details the design and construction of a new gas permeation testing system that can operate up to 300°C and safely handle a flammable gas, like H_2.

5.1 Equipment Design

Several researchers have published permeation results on sol-gel derived silica and metal doped silica membranes in a temperature range of 100-500°C using isobaric (constant pressure, variable volume) permeation equipments [1-7]. The permeabilities are calculated based on the volumetric flow rate of the permeate stream. However, the papers do not explicitly describe the modifications needed to enable high temperature testing, nor do they address the masking or mounting techniques of the membranes to enable testing under such aggressive conditions. This chapter details the challenges and considerations in the design of an isochoric (constant volume) high temperature permeation equipment as well as the masking technique for microporous film characterization. In an isochoric system, pressure rise due to accumulation of gas in a constant

volume is measured. Masking refers to a method of attaching a membrane to the permeation test cell such that the only available path for passage of gas remains through the membrane and the surrounding region is made impermeable to gases.

The basis of a constant volume pressure rise permeation system is well-known in literature [8,9]. In principle, in this method, following a thorough evacuation of the entire system, gas at a constant pressure is fed and maintained on the upstream face of the membrane while the downstream is under vacuum. As gas permeates through the membrane due to the pressure driving force, pressure in the downstream reservoir increases. This rate of increase in pressure (dP/dt) in the downstream is recorded in the range 0-10 torr and used to calculate the gas permeability. The maximum downstream pressure is <0.1% of the upstream pressure of typically more than 50psia and this allows the assumption of a constant pressure drop across the membrane.

In standard permeation systems, all the components are maintained at the desired temperature of operation and can withstand a maximum temperature of 60°C only. The presence of heat sensitive electrical components imposes restrictions on the operating temperature. Relocation of the sensitive electrical parts (downstream transducer signal conditioner) to outside the permeation enclosure can enable raising the operating temperature. To achieve very high operating temperatures, further modifications are necessary. A schematic of the newly designed high temperature permeation system is shown in figure 14.

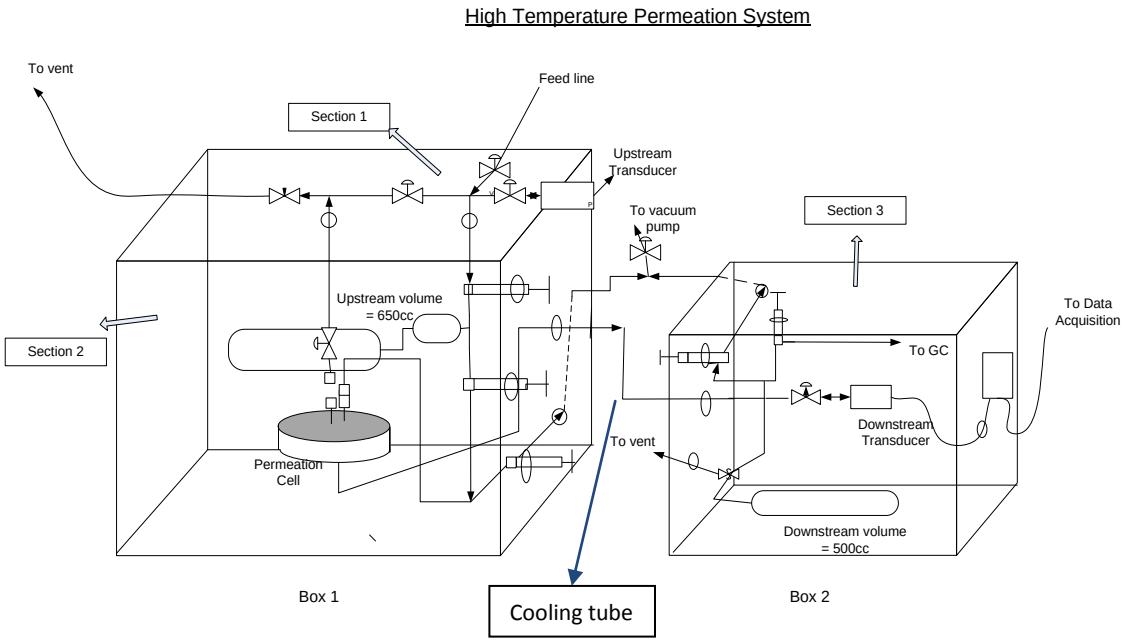

Figure 14. Schematic of high temperature gas permeation system that can enable operations up to 300°C

In the majority of literature available on high temperature gas permeation testing, only the membrane module is placed in a furnace at desired temperatures. This eliminates the possibility of damage to the electrical components due to the excessive heat. Similarly, in the present work, the constant volume permeation system designed (figure 14) is segregated into three sections. The system consists of two insulated boxes, 1 and 2.

- Section 1 is located above box 1 and always remains at ambient temperature. It comprises the gas feed line, upstream transducer (Sensotec Model Z, absolute 0-1000psia), mixed gas retentate line and vent line.
- Section 2 leads the feed line into box 1 and comprises the upstream volume and the permeation cell. Section 2 is maintained at the desired operating temperature via a heating mechanism. Heavy insulated heating tapes, controlled by PID tuned benchtop controllers (Omega®) and K-type thermocouples have been employed for controlling the temperature of

this section. The components of section2 would be carefully heat wrapped with the heating tapes and additional insulation tape and the thermocouples would be inserted to detect surface temperatures in this section. Section 2 is connected to section 3 (located in box 2) through stainless steel tubing to cool the permeate (Appendix II).

- Section 3 has the downstream volume with downstream transducer (Baratron, 0-10 torr), a pressure relief valve and a line connecting to a gas chromatograph. Section 3 is independently maintained at 35°C. The pressure relief valve vents gas at pressures greater than 30psia in case of an unexpected pressure surge resulting from membrane failure thereby protecting the downstream transducer from damage.

The upstream and downstream volumes are also connected to a vacuum pump (BOC Edwards model RV3) for evacuation. The maximum operating temperature for the system is 300°C as the maximum temperature that the Kalrez® (Du-Pont) O-rings used, for sealing the permeation cell, can withstand is 315°C.

5.2 Principle of Operation

After evacuation of the entire system, gas is fed into the upstream volume at ambient temperature at a pressure calibrated with desired pressure at the operating temperature and section 2 is heated to the desired temperature of operation. The permeation cell and downstream volume are isolated from the upstream by the feed valve and maintained under vacuum. Once the feed valve is opened, transport of gas through the membrane occurs at the desired temperature. The permeate flows through section 2, cools in the steel tubing between box1 and box2 and starts accumulating in the downstream volume in section 3. Section 3 is maintained at 35°C. The rise in pressure in the downstream volume as a function of time dp/dt is recorded and this data is used to calculate the permeability of the gas through the membrane film at the operating temperature and pressure.

Based on preliminary permeation test results extrapolated to higher temperatures, the upstream and downstream volumes were calculated. The upstream volume needed to be small enough to prevent explosion in case of a hydrogen leak and large enough to maintain a constant Δp across the membrane. The downstream volume was required to be large enough to enable accurate data collection of the fastest penetrant and small enough to sustain a constant Δp. Based on the above constraints, the upstream volume was estimated to be 650cc and the downstream volume, 500cc. The exact value of the downstream volume was measured to be 560cc, including fittings (with the help of a calibrated volume).

5.3 Materials of construction

Enclosure 1 is a 316/316L stainless steel box lined with very high temperature silica-alumina-magnesia insulation. Box 2 was made of wood and insulated with thick layers of fiberglass. All fittings were made of 316/316L stainless steel (SS) to ensure stability against high temperature and hydrogen environment. SS bellows UW series® valves (including long handle valves) were used to provide perfect sealing and ease of handling. These valves have a welded body seal and are rated to 482°C. Additionally, all fittings were used with SS VCR (Swagelok®) face seal connections to provide leak proof operation. A high temperature pipe thread sealant (Coplatite®), National Engineering Products Inc.) was used to seal NPT connections in the upstream volume ballasts.

Hydrogen embrittlement (or hydrogen grooving) is the process by which various metals, most importantly high strength steel, becomes brittle and crack following exposure to hydrogen [13,14]. Steels with an ultimate tensile strength of less than 1000MPa or hardness of less than 30 Rockwell C are essentially insensitive to hydrogen embrittlement. Stainless steel alloys 316/316L, of which the ballasts and fittings are made, have an ultimate tensile strength of 515

MPa (316) and 485MPa (316L) [13-15]. SS 316L tests 491MPa at 316°C. SS 316L has a maximum Rockwell C hardness of 20. Therefore, hydrogen embrittlement is not expected to pose any problems in the system.

Heavy insulated heating tapes (Omega® FGH051-060-LSE) , which are ideal for use on conductive surfaces like steel, were used for maintaining respective temperatures in sections 2 and 3. For accurate temperature control, the heating tapes were controlled via K-type thermocouples (Omega® KMTXL-062[G]-[6]) and PID tuned benchtop temperature controllers (Omega® CSi32k).

Detailed design of the stainless steel machined permeation cell is available [8]. This cell permits measurement of flux through materials of varying areas for both pure and mixed gas feeds. The cell is sealed by a pair of O-rings and 6 stainless steel bolts. For high temperature conditions, the selection of the O-ring material was critical and Kalrez® O-rings (DuPont) that are rated to 315°C were selected.

5.4 Precautions for H_2 testing:

Hydrogen is a highly flammable gas i.e. in some range of concentration, a H_2 – air mixture can combust if there is a source of ignition. This range of concentration or the flammability limits for hydrogen in air are 4-75 volume or mole% H_2 in air, at room temperature [15-17]. The lower limit is called the lean flammability limit (LFL). This range widens as temperature increases. Increase in pressure does not affect the lower limit but greatly affects the upper limit.

The new permeation system was designed such that if all the hydrogen contained in the upstream volume leaked out into box 1 and there was a source of ignition (like a spark caused from the heating tapes or some kind of electric discharge), the contents in the box would not undergo

combustion. In other words, the leaked hydrogen air mixture in box 1 should have hydrogen to air volume % of less than the LFL at that temperature. The mixture can auto-ignite if it reaches 585°C which is beyond the operating limit of the system of 300°C. The following table presents calculations of the flammability value (volume %) of H_2-air mixtures that would be formed if all H_2 from the upstream volume leaked into box1 (H_2 at operating temperature of section 2 and air at ambient conditions) [15-17]. From table 5, it is clear that *the new system is safe for testing H_2 up to 150 psia feed pressure at temperatures up to 300℃.*

Table 5. Flammability values of H_2 (volume%) in air in case of a total H_2 leak in box 1 of schematic shown in figure 14. Values in the shaded area with red text indicate unsafe operating conditions.

T (°C)	25	100	200	300
P_{up} (psia)				
20	0.51	0.41	0.32	0.27
50	1.26	1.01	0.80	0.66
100	2.49	2.00	1.58	1.31
150	3.68	2.97	2.35	1.95
200	4.85	3.92	3.11	2.59
250	5.99	4.85	3.86	3.21
300	7.11	5.76	4.60	3.83
LFL%	**4.00**	**3.76**	**3.44**	**3.12**

Helium leak tests were performed to ensure that no leaks were present in the fittings. This is extremely important in order to provide safe operation with flammable gases as well as for accurate data collection. No He leaked out of the system when the operation temperature was at the maximum value of 300°C. Since He is a smaller molecule than H_2, we can be assured that no H_2 would leak out of the system as well. Periodic leak tests will be performed with He.

5.5 Experimental technique:

Membrane Masking technique: Several techniques of masking films in permeation cells are known [8,9]. These robust techniques are applicable for low and high pressure environments and polymeric films. High temperature environments demand use of thermally stable materials for the mask. A disc of glass wool can be used as a cushion to support the silica membranes. The glass wool layer can be secured to the lower half of the permeation cell with an impermeable high temperature polyimide tape (3M™ Kapton® Polyimide Film Tape 5413 Amber, 2.7 mil (0.07 mm) with a silicone adhesive, flame retardant, chemical and radiation resistant), which has a hole punched in the center to match the diameter of the membrane film. A thicker version (5mil) of the same tape is also available from Kaptontape.com and both are rated to 260°C. A flat membrane film would then be placed in the hole, with the downsteam under vacuum. High temperature epoxy will be applied around the film to provide an impermeable seal between the membrane, the polyimide tape and the glass wool layer (figure 15). The tape will also be covered with epoxy to make it impermeable as well as to enable data collection in 260-300°C.

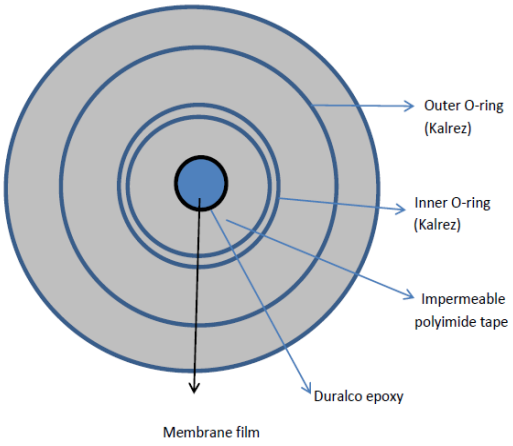

Figure 15. Top view of lower half of permeation test cell, after masking a silica membrane film

The permeation cell can then be closed uniformly by bolting the six stainless steel bolts (32 lb_f) with steel washers. The cell would be heated at 120°C for 2 hours and 180°C for 4 hours

(manufacturer recommended) to effect complete curing of the epoxy, with the downstream under vacuum. The mask gets sealed with a pair of Kalrez® O-rings and the only path available for gas permeation remains through the available area on the membrane. The area of permeation on the membrane films masked in this way is usually 0.5-1.0cm^2. The thickness of the membrane is measured with a micrometer (0.1mil accuracy) and the area of permeation is measured using a software named Scion Image®.

Gas permeation testing: After masking the membrane into the system, the entire system is thoroughly evacuated for 24-48 hours to degas the system. First, a leak rate is measured by monitoring the downstream pressure rise while the system remains evacuated. For inorganic membranes in high temperature operating conditions, the leak rate is usually a negligible fraction of the permeation rate of the slowest penetrant.

In each gas permeation experiment, the time lag and rate of rise in downstream pressure in the range 0.2 to 10 torr is recorded, at a known feed pressure and temperature. From the obtained data, the steady state data is used to calculate the permeability of the penetrant. Steady-state is assumed to be attained after 10 time lag periods. An apparent diffusion coefficient can be estimated from the steady state permeation data. For each experiment, a second run is performed by evacuating the downstream in steady state to verify that the rate of rise in pressure remains the same as in the previous run. A time lag is not observed in the second run as the system is already under steady state conditions. The calculated permeability includes correction for leaks by subtraction of the leak rate from the measured permeation rate. Before a different gas penetrant is studied, the entire system is evacuated for atleast 12 hours.

The steady state flux (dp/dt) is used to calculate the permeability (in 10^{-10}Barrer) using the following expressions:

$$P = \frac{N_A l}{\Delta p.A} = 3.045 \frac{\frac{dV(STP)}{dt}.l}{\Delta p.A} \quad (8)$$

$$\frac{dV(STP)}{dt} = \frac{\frac{dP}{dt}.Vd.273}{760.(T+273)} \quad (9)$$

where dp/dt = rate of increase in permeate pressure (torr/sec), V_d = downstream volume (cm^3), T = temperature (Kelvin), l= thickness of the membrane (mils), Δp = pressure drop across the membrane (psia), A= area of permeation ($pixel^2$).

5.6 Gas permeation tests on standard membranes

To exhibit the operability of the newly constructed system, gas permeation tests were performed on two standard membranes- PDMS and a polyimide. Since it was possible to obtain large membrane areas in both these cases, no masking was required and a large membrane film was directly sealed between the two O-rings in the permeation cell. The gas permeation results are presented as follows.

1. *Permeability of Helium through polydimethylsiloxane membrane film* (rubbery polymeric membrane): Permeation tests were conducted with He, through a PDMS membrane film. The tests were conducted at 50, 80, 100 and 120°C. The obtained variation in permeability is presented in figure 16. From this data, the activation energy for permeation and pre-exponential factor (equation 6) for He through PDMS were calculated. Area=$30cm^2$, thickness =6.9mils.

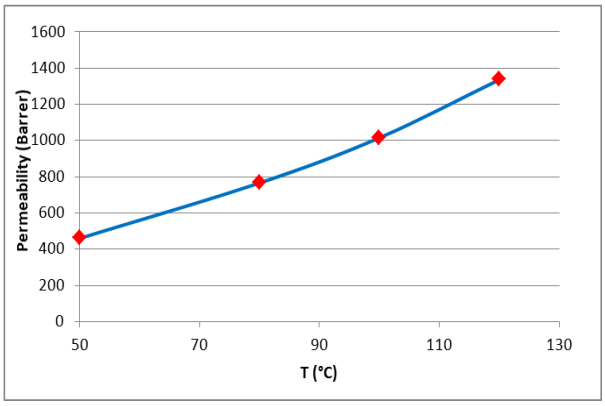

Figure 16. Permeability of He through polydimethylsiloxane in the temperature range 50-120°C, at 57 psia pressure difference

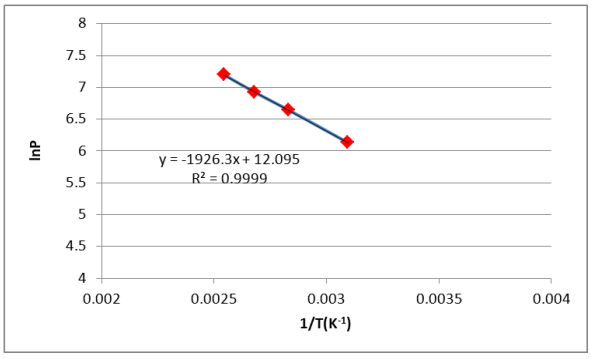

lnP (vs) 1/T Arrhenius plot for PDMS membrane film; Ep= 16kJ/mol, P_0= 179000Barrer

2. *Permeability of CO_2 through a polyimide membrane* (glassy polymeric membrane): A polyimide membrane film, received from Idaho National Labs, was tested. The exact chemical structure of this material is unknown due to proprietory rights. Nevertheless, this material could be tested for CO_2 permeability in the temperature range 80-200°C. The data is presented in figure 17. Area=30cm^2, thickness = 1.65mils. The membrane changed color after 200°C. This indicated slow thermal degradation of material and further gas permeation tests were not conducted.

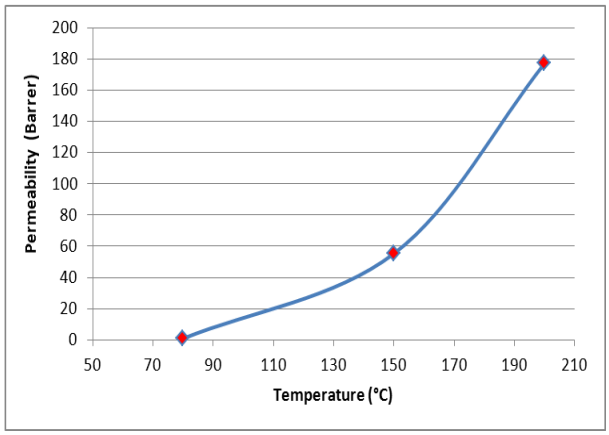

Figure 17. Permeability of CO_2 through a polyimide membrane film in the temperature range 80-200°C, at 100psia pressure difference

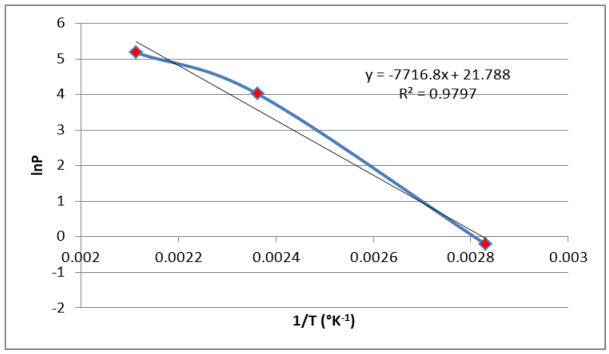

lnP (vs) 1/T Arrhenius plot for polyimide membrane film; Ep= 64.16kJ/mol,P_0= $2.9x10^9$ Barrer

3. *Silica membranes*: The PDMS derived silica membranes are thermally stable up to 390°C (in air). These membrane films require robust masking (as described in section 5.5.) and will be tested in the new system in future, in the temperature range 50-300°C with He, H_2, CO_2 and N_2.

References:

1. Kanezashi, M., Asaeda M., *Hydrogen permeation characteristics and stability of Ni-doped silica membranes in steam at high temperature,* Journal of Membrane Science, 2006, **271**(1-2), 86-93.
2. Yoshida, K., et al., *Hydrothermal stability and performance of silica-zirconia membranes for hydrogen separation in hydrothermal condition,*Journal of Chemical Engineering of Japan, 2001, **34**(4), 523-530.
3. Battersby, S., et al., *Performance of cobalt silica membranes in gas mixture separation,* Journal of Membrane Science, 2009, **329**(1-2), 91-98
4. Barboiu, C., et al., *Structural and mechanical characterizations of microporous silica-boron membranes for gas separation,* Journal of Membrane Science, 2009, **326**(2), 514-525
5. de Vos, R.M. and H. Verweij, *High-selectivity, high-flux silica membranes for gas separation,*. Science, 1998, **279**(5357), 1710-1711.
6. Hassan, M.H., et al., *Single-Component and Mixed-Gas Transport in a Silica hollow-Fiber Membrane,* Journal of Membrane Science, 1995, **104**(1-2), 27-42
7. Way, J.D. and D.L. Roberts, *Hollow Fiber Inorganic Membranes for Gas Separations,* Separation Science and Technology, 1992, **27**(1), 29-4
8. Moore, T., et.al., *Characterization of low permeability gas separation membranes and barrier materials: design and operations,* Journal of Membrane Science, 2004, 245, 227–231.
9. Damle, S., Koros, W.J., *Permeation equipment for high pressure gas separations,* Ind. Eng. Chem. Res., 2003, 42(25), 6389-6395.
10. O'Brien, K.C., et.al., *New technique for the measurement of multicomponent gas transport through polymeric films,* Journal of Membrane Science, 1986, 29(3), 229-238

11. Koros, W.J. and G.K. Fleming, *Membrane-Based Gas Separation*, Journal of Membrane Science, 1993, **83**(1), 1-80
12. Molyneux, P., *Permeation of gases through microporous silica hollow-fiber membranes: Application of the transition-site model*, Journal of Membrane Science, 2008, **320**(1-2), 42-56
13. http://www.sandmeyersteel.com/images/316-316L-317L-Spec-Sheet.pdf
14. http://www.azom.com/Details.asp?ArticleID=2382
15. Perry, R.H., Green, D.W., *Perry's Chemical Engineer's Handbook,* 7th edition,1997, McGraw Hill
16. Alcock, J.L., et.al., *Compilation of existing safety data on hydrogen and comparative gases*, May 2001
17. College of the Desert, Palm Desert, CA, USA, *Hydrogen Fuel Cell engines and related technologies*, Module 1, December 2001

Chapter 6. Suggestions for Future Work

Fabrication of inorganic silica membranes from polydimethylsiloxane is an invention that has been demonstrated, as described in chapters 2-4 in this thesis. Acceptable gas separation performance in 35-80°C temperature range has been achieved but more extensive data needs to be collected in order to determine high temperature performance and membrane-penetrant interaction properties. Therefore, this chapter describes the work planned for furthering the current research.

Strategy and optimization of the membrane fabrication process consumed about 50% of the total time of this research. In result, the ideal fabrication parameter values to obtain defect free flat silica and silica-titania membranes from PDMS were determined. One of the fabrication parameters, the O_2 flow rate, was found to cause variations in the gas transport properties of the silica membranes. It changes the average pore size of the membranes thereby changing the corresponding activation energies and selectivites. Hence, this parameter needs attention and it can enable tuning of micromorphology of the membranes. 30ml/min and 50ml/min were two values that have been used until now. Membranes created at 50ml/min show higher He and H_2 permeabilities and are expected to have smaller pores (higher activation energies). It is proposed that membranes created at 70ml/min O_2 will be even denser and provide excellent high temperature H_2-CO_2 separation performance.

Building the high temperature permeation system, gathering high temperature materials and completing auxiliary tests like downstream volume measurement, He leak tests for safety and pressure relief valve calibration consumed 20% of time. The choice of the high temperature masking tape (3M™ Kapton® 5413) and high temperature epoxy (Duralco® 4703) were also critical to the progress of this research.

It is planned to mask silica membranes fabricated at 30, 50 and 70 ml/min O_2, into the new system and collect gas permeation data for each as tabulated in table 6. It is proposed to test Δp = 50, 70 and 100psia because at ~90psia (figure 12), the silica membranes become H_2 selective even at 35°C.

Table 6.Plan for collection of gas permeation data through silica membranes, in new system

Gas	Temperature (°C)	Pressure Δp (psia)
He	50, 100, 150, 200, 250, 300	50, 70, 100
H_2	50, 100, 150, 200, 250, 300	50, 70, 100
CO_2	50, 100, 150, 200, 250, 300	50, 70, 100
N_2	50, 100, 150, 200, 250, 300	50, 70, 100

From the above data, it will be possible to calculate pure gas permeability and selectivity values. Additionally, Arrhenius plots (lnP (vs) 1/T) will yield the activation energies, $E_{p,}$ and pre-exponential factors, P_0, for different penetrants. A hypothetical pore in an amorphous silica membrane is made up of pore constrictions (which determine the activation energy) and free volume regions (open galleries that sorb the gas molecule).

Analysis of the data for Ep (vs) kinetic diameter should yield a line with a positive slope since a larger penetrant like N_2 would need higher energy to transport through the pores of the membrane than other penetrants, if sorption effects are negligible. In fact, however, since sorption effects will certainly enter the picture, the behaviour of CO_2 may not correlate so simply and it will presumably show an apparent Ep value lower than expected.

The results will also clarify how variation in O_2 flow rate, during fabrication, causes variations in the micromorphology of the silica membranes and this will be explored as a function of Ti content in the silica membranes as well. It is expected that higher the O_2 flow rate, smaller will be the pores and higher will be activation energies of permeation (E_p's). By determining the sorption enthalpies (ΔH_s), the true activation energies for diffusion (E_d) can be determined, and this will explain any odd effects such as noted for CO_2 when permeability is considered without factorization into diffusion and sorption components.

The next task would be to fabricate Silica-Titania membranes at 30, 50 and 70 ml/min O_2 flow rate, according to the already optimized protocol, and subject them to gas permeation tests according to table 6. It is expected that Ti doped silica membranes will have lesser affinity for CO_2 and provide H_2/CO_2 separation performance better than pure silica membranes.

Finally, permeation and separation of mixed gas H_2-CO_2 would be tested through the silica and silica-titania membranes. It is planned to test H_2:CO_2 = 3:7, 1:1 and 7:3 mixtures. In industry, the gas mixture exiting from the high temperature shift reactor usually has a H_2:CO_2 ratio of 3 or 4. It is proposed to install a membrane unit after this reactor. If we can achieve good separation performance for a 1:1 mixture at 300°C, use of such membranes for separation in the water-gas shift process would be easier. Testing mixed feed mixtures requires installation of a gas-chromatograph (GC) in the permeation system. The new system does have provision for a GC and calibration of the GC for H_2-CO_2 needs to be performed prior to mixed gas permeation tests.

For use in the water gas shift process, it is important that the silica membranes show consistent gas separation performance even in the presence of steam. Hence, it is also planned to test the gas separation performance of the silica and silica-titania membranes after exposure to steam. These results would be compared with those of membranes unexposed to steam. It is expected that there

might be a decrease in the permeabilities of the gases, due to adsorption of H_2O in the micropores of the membranes but depending upon the pore size distribution of the membranes, the selectivity may decrease or remain unaffected. The micropore size would get reduced due to interactions of the membrane with –OH groups of H_2O. If there is a small fraction of larger pores in the membranes, they would shrink to microporous range. However, since all surface –OH groups have been removed in the thermal oxidation process during fabrication (very small –OH peak in FTIR in figure 6b)), it is believed that PDMS derived silica membranes would have minimal interaction with steam. Since no preliminary tests have been conducted on this subject, it is difficult to predict the effect of steam on the newly developed membranes. In accordance with literature on Sol-Gel, it is also hypothesized that Silica-titania membranes would exhibit higher hydrothermal stability than pure silica membranes due to difference in polar nature of the material and a reduced tendency to interact with steam. The work proposed in this chapter is part of my ongoing Ph.D. program and is expected to complete by Spring 2013.

References:

1. Molyneux, P., *Permeation of gases through microporous silica hollow-fiber membranes: Application of the transition-site model,* Journal of Membrane Science, 2008, **320**(1-2), 42-56
2. Boffa, V., D.H.A. Blank, and J.E. ten Elshof, *Hydrothermal stability of microporous silica and niobia-silica membranes.* Journal of Membrane Science, 2008. **319**(1-2): p. 256-263.
3. Kanezashi, M. and M. Asaeda, *Hydrogen permeation characteristics and stability of Ni-doped silica membranes in steam at high temperature.* Journal of Membrane Science, 2006. **271**(1-2): p. 86-93.
4. Yoshida, K., et al., *Hydrothermal stability and performance of silica-zirconia membranes for hydrogen separation in hydrothermal conditions.* Journal of Chemical Engineering of Japan, 2001. **34**(4): p. 523-530.
5. Battersby, S., et al., *Hydrothermal stability of cobalt silica membranes in a water gas shift recator, Separation and Purification technology*, 2009. **66**: p. 299-305

Appendix I Membrane separation in water gas shift process

The water gas shift reaction involves reaction of CO with high temperature steam (350-300°C) to produce H_2 and CO_2. The process runs in a pair of high temperature and low temperature shift reactors (HTS and LTS). The reaction is exothermic in nature. This section presents my calculations to show that installation of a hydrogen selective membrane between the two water gas shift reactors can provide enhanced efficiency of the overall process. Some realistic assumptions have been made. The motivation behind these calculations was to determine the H_2/CO_2 selectivity of a membrane that is required for the process.

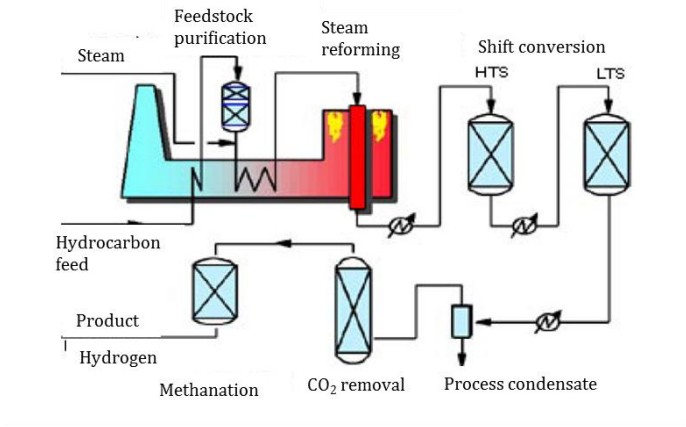

1. Operate HTS at conditions that favor kinetics and thermodynamics at 350°C
   $\ln K = 4587.3/T - 4.3113$
2. H_2 selective membrane between HTS and LTS
3. Membrane separation before LTS increases conversion in LTS
4. Rate of reaction in LTS is higher due to higher driving force- lower concentration of products entering. Higher rate allows a smaller volume of reactor to be used.

The product stream from LTS , after membrane separation, is CO_2 rich and downstream CO_2 removal becomes more efficient.

Figure 18. Schematic of industrial hydrogen production process showing the steam reformer, water-gas shift reactors and downstream CO_2 removal sections (figure taken from making-hydrogen.com). Description of how installation of a membrane unit in between the HTS and LTS can provide advantages.

Calculations:

'i' refers to moles in initial and 'f' refers to moles in final states.

1. Steam methane reforming reaction (800°C):

Assumptions:

1. 4:1 ratio of steam to reactant natural gas enters the steam reformer
2. Due to high temperature that would favor forward direction of the endothermic reaction, 100% conversion of methane is assumed.

	CH_4	+ H_2O ↔	CO	+ $3H_2$	ΔH=206 kJ/mol
i	1	4	0	0	
f	0	3	1	3	

2: Water-gas shift reaction

$CO + H_2O \leftrightarrow CO_2 + H_2$ ΔH= - 41.2 kJ/mol

Variation of equilibrium constant with temperature lnK= - 4.3113+ 4587.3/T [Ref.]

[Ref]: Elementary principles of Chemical Processes, Ronald Rousseau

This reaction is carried out in two stages- High Temperature Shift and Low Temperature Shift

2.1: HTS at 350°C, K=21.156, the mixture exiting from the steam reformer enters the HTS.

$CO + H_2O \leftrightarrow CO_2 + H_2$

i	1	3	0	3
f	1-χ	3-χ	χ	3+χ

$\mathbf{K=[CO_2]_f[H_2]_f / [CO]_f [H_2O]_f}$

χ= 0.9185

Hence, concentrations at the exit of HTS are as follows

	CO	+	H_2O	↔	CO_2	+	H_2
i	1		3		0		3
f	0.0815		2.0815		0.9185		3.9185

Mol %(dry basis) 79.7% H_2, 18.7%CO_2, 1.66%CO

CO conversion = 91.85% $[H_2/CO_2]_{EXIT}$ = 4.27

2.2a):

LTS at 200°C (lower limit of temperature due to water dew point at reactor conditions)

K=218.55

	CO	+	H_2O	↔	CO_2	+	H_2
i	0.0815		2.0815		0.9185		3.9185
f	0.0815-χ		2.0815-χ		0.9185+χ		3.9185+χ

χ= 0.07256

	CO	+	H_2O	↔	CO_2	+	H_2
i	0.0815		2.0815		0.9185		3.9185
f	0.009		2.009		0.991		3.991

CO conversion in LTS= 89.1%

Concentrations at exit of LTS (mol%)

CO=0.13

H_2O= 28.7

CO_2= 14.16

H_2=57

Stream exiting from LTS is H_2 rich, in the absence of any membrane separations.

2.2.b):

A hydrogen selective membrane unit has been installed in between the HTS and LTS.

LTS operating at 200°C. K=218.55

Lesser amount of H_2 enters the LTS.

Amount of H_2 entering the LTS depends on the selectivity of the membrane unit before.

Assumption: Membrane unit is impermeable to CO and H_2O.

In LTS,

	CO	+	H_2O	$\leftrightarrow$	CO_2	+	H_2
i	0.0815		2.0815		0.9185		x
f	0.0815-χ		2.0815-χ		0.9185+χ		x+χ

Assumption: 99% conversion of CO in the LTS is attractive

$0.99=[0.0815- (0.0815-\chi)]/0.0815$

$\Rightarrow\chi= 0.080685$

Now,

$218.55=[(x+0.080685)*1]/[0.000815*2]$

$x=0.2755$

Therefore, H_2 removed in the membrane unit = H_2 at HTS exit – H_2 at LTS entrance

$=3.9185- 0.2775=3.643$

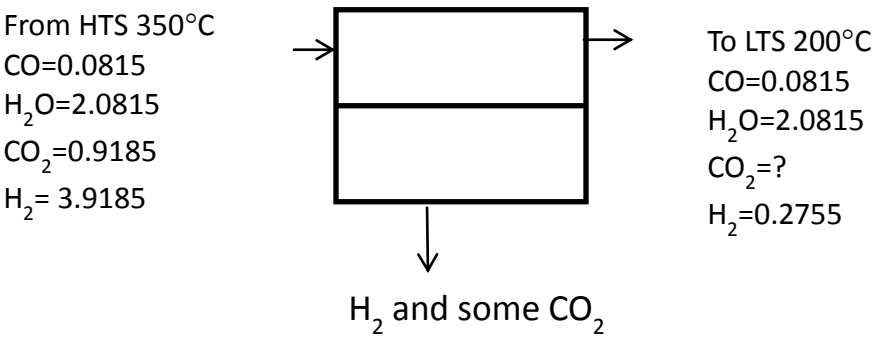

Assumptions: 1. Cross flow pattern

Permeate stream from membrane unit:

Purity of permeate stream= $n_{H2}*100/(n_{H2}+n_{CO2})$ (10)

Selectivity of membrane unit = $[n_{H2}/ n_{CO2}]_{permeate}/ [n_{H2}/n_{CO2}]_{feed}$ (11)

$[n_{H2}/n_{CO2}]_{feed}$= 3.9185/0.9185=4.27

Using equations 10 and 11, for the permeate stream,

Desired purity of permeate stream Moles of gas in permeate stream	90%	99%	99.9%
H_2	3.643	3.643	3.643
CO_2	0.4048	0.03676	0.00364
Membrane selectivity needed when feed ratio=4.27	2	23	234
Membrane selectivity needed when upstream is well mixed and feed ratio=2.33	4	43	430

2.2 c):

Assumption: A membrane unit with H_2/CO_2 selectivity of 23.2 has been installed between the HTS and the LTS.

LTS operating at 200°C. K=218.55

	CO	+	H_2O	$\leftrightarrow$	CO_2	+	H_2
i	0.0815		2.0815		0.88174		0.2755
f	0.0815-χ		2.0815-χ		0.88174+χ		0.2755+χ

$\Rightarrow\chi$=0.08107 CO conversion= 99.47%

	CO	H_2O	CO_2	H_2
f	0.00043	2	0.96281	0.356

In the presence of a membrane unit, concentrations of products entering LTS are lower, as compared to the values without membrane separation. This leads to higher CO conversion and higher rate of conversion in the LTS.

For a reversible catalyzed reaction, like the water-gas shift-reaction, the rate increases when the concentration of the products in a mixture is low i.e. driving force for forward reaction is high. Hence, installation of a H_2 selective membrane in between the HTS and the LTS would reduce the concentration of product H_2 entering the LTS, thereby enhancing the rate of reaction in the LTS. Higher rate of reaction also implies that a smaller reactor volume is needed.

Stream exiting from LTS (mole%)

[CO]=0.01% $[H_2O]$=60.25% $[CO_2]$=29% $[H_2]$=10.7%

Stream exiting from the LTS is CO_2 rich, in presence of a membrane unit between the HTS and LTS. This makes downstream CO_2 absorption more efficient.

Appendix II Length of cooling tube in high temperature system

In the design of the high temperature permeation system described in chapter 5, there exists stainless steel tubing between section 2 and section 3. The function of this tube is to cool the hot permeate before it reaches section 3. This section presents heat transfer calculations to determine the minimum length of SS tubing needed in the high temperature permeation system.

Length of tube connecting box 1 to box 2 to cool permeate

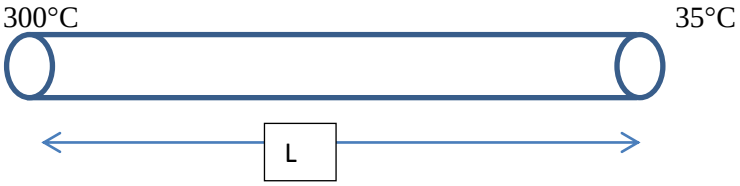

For a silica membrane fabricated at 50 ml/min O_2, membrane properties:

P_{H2} (300°C) = 2860 Barrer (Δp=49.7psia) is estimated. Thickness = 8mils. Area= 1cm^2

SS 316/316L Tube length L= to be determined, inner diameter= 0.178", outer diameter=0.25"

$$P = 2860 \times 10^{-10} \quad \frac{cm^3(STP).cm}{cm^2.sec.cmHg} = \frac{(\frac{dV}{dt})_{STP}.l}{\Delta p.A}$$

$$\Rightarrow (dV/dt)_{STP} = 3.6165 \times 10^{-3}\ cm^3_{(STP)}/s \qquad (12)$$

At STP, 760torr.(dV/dt) = (dn/dt).R.273

At 35°C (temperature of permeate at downstream), $(dp/dt).V_d = (dn/dt)R.308$

$$\Rightarrow \frac{\frac{dP}{dt}.V_d}{760\text{torr}.\left(\frac{dV}{dt}\right)_{STP}} = 1.1282$$

For V_d= 500cc, we obtain dp/dt = 0.0062 torr/sec.

And, (dn/dt) = $(dp/dt)V_d/RT = 1.614 \times 10^{-4}$ mol/sec

Volumetric flow rate through cooling tube

$$\frac{dV}{dt} = \frac{\frac{dn}{dt}*M}{\rho_{H2(168°C)}} = \frac{(1.614*10^{-4}*2*10^{-3})}{0.05462} = 5.91\ cm^3/s$$

Velocity U= (dV/dt) /A= $\frac{5.91}{(\pi\ di^2/4)} = 36.8\ cm/s$

Nre= 7.7145×10^{-6}

Total heat transferred during passage of gas through cooling tube

$q_{total} = h_g.A_i(T_g-T_1) = 2\pi kL(T_1-T_2)/\ln(r_o/r_i) = h_{air}.A_o(T_2-T_{amb})$

Addition gives $T_g-T_{amb} = \frac{q}{h_g.A_i} + \frac{q}{(2\pi kL)/\ln(r_{o/r_i})} + \frac{q}{h_{air}.A_o}$

$$q = \frac{\Delta T_{ln}}{\frac{1}{h_g.A_i} + \frac{\ln\left(\frac{r_o}{r_i}\right)}{2\pi kL} + \frac{1}{h_{air}.A_o}}$$

1. Heat transfer resistance due to convection on inner surface of tube

   q_w= constant, Re<5×10^5, 0.6<Pr<50

   $N_{Nu} \approx 3.66$ for when d<<L

$$\frac{h_g \times 0.178 \times 2.54 \times 10^{-2}}{0.251} = 3.66 \qquad \Rightarrow h_g = 203.19 W/m°C$$

$$\frac{1}{h_g.A_i} = \frac{1}{203.19*\pi.di.L} = \frac{0.3465}{L} \text{ units}$$

2. Heat transfer resistance due to conduction through tube walls

$$\frac{\ln(r_o/r_i)}{2\pi kL} = \frac{\ln\frac{0.25}{0.178}}{2\pi*0.25L} = \frac{0.21538}{L} \text{ units}$$

3. Heat transfer resistance due to convection on outer surface of tube

$$\frac{1}{h_{air}.A_o} = \frac{1}{40*\pi*0.25*2.54*0.01L} = \frac{1.253}{L} \text{ units}$$

4. $Q = (dm/dt).\ Cp.\ (T_{in}-T_{out}) = 3.23 * 10^{-4} * 10^{-3} * 14.5 * 10^{3} * (300 - 35) = 1.24027W$

$$\Delta T_{ln} = \frac{(300-25)-(35-25)}{\ln(300-25/35-25)} = \frac{265}{\ln(26.5)} = 80.863°C$$

$$1.24027 = \frac{80.863}{\frac{0.3465}{L} + \frac{0.21538}{L} + \frac{1.253}{L}}$$

L= 2.78cm

Tubing of length 34" has been used in the high temperature permeation system to ensure that the permeate gas (H_2) cools before it reaches the downstream volume. This is done to prevent damage to downstream transducer as well as to ensure that the permeate loses its potential to undergo inflammation at room temperature.